PETROLOGIC AND PETROGRAPHIC ANALYSIS OF ANCIENT SUBMARINE HYDROCARBON SEEP DEPOSITS (LATE CRETACEOUS) FROM THE TEPEE BUTTES OF COLORADO

By
Julia Anderson

A thesis submitted to the department of Geology at
Gustavus Adolphus College
in partial fulfillment of the requirements for the degree of
Bachelor of Arts

May 2006

ABSTRACT

PETROLOGIC AND PETROGRAPHIC ANALYSIS OF ANCIENT SUBMARINE HYDROCARBON SEEP DEPOSITS (LATE CRETACEOUS) FROM THE TEPEE BUTTES OF COLORADO

By:
Julia Anderson
Under the supervision of Dr. Russell Shapiro

The Tepee Buttes (~76 Ma) are ancient methane seep deposits of the Cretaceous Interior Seaway. They formed from methane-rich fluid seeping out of the underlying Pierre Shale and Niobrara formations during early Laramide faulting. Similar to modern seeps, these carbonates most likely formed from geochemical changes brought on by methanotropic bacteria (oxidation of methane) and sulfate reducing bacteria.

The Tepee Buttes carbonates consist of five different lithofacies: (I) vuggy intrapelsparite with complex cements as well as articulated and disarticulated clams; (II) dense coquina of articulated lucinid clams in vuggy intrapelsparite; (III) clams in micrite; (IV) limestone concretions; and (V) vuggy peloidal intraclastic microbialite. 106 buttes were analyzed for different lithologic facies near Colorado Springs, CO. Contrary to earlier studies that suggest a concentric arrangement of lithofacies around a central vent core, we found evidence of horizontal bedding of limestone separated by thin shale layers.

Samples were analyzed for petrographic fabrics using petrographic and cathodoluminescence microscopes as well as stable isotopes. These data provide evidence for determining a series of primary to late stage diagenetic features recording fluid diagenesis. Petrofabrics include pelmicrite, intrapelmicrite and intrapelsparite, and fringing, isopachous, botryodal and late stage spar cements. Petrographic characteristics of lithofacies I include intrapelsparite and intrapelmicrite with fringing, botryodal, isopachous and spar filling cements. Lithofacies II and III consist of sparitized shells filled in with spar or micrite. III is pelmicrite and II is intrapelsparite and voids with a thin (0.1mm) fringe cement and thick (1.25mm) botryoids. IV consist of a homogenous gray micrite. V contains intrapelsparite with spar filled voids. δ^{13} C isotope ratios for the microbial peloids range from -36.77 to -10.50 ‰ PDB. The primary micrite with siliciclastic grains range from -38.58 to -12.07. Values for the intraclasts within the primary micrite are -35.86 to -7.33. The primary cements include yellow calcite fringe with δ^{13} C values of -39.28 to -36.98, botryoidal and isopachous cements with δ^{13} C values of -48.73 to -34.95. During the latest stages, blocky calcite spar cement filled in the remaining void space and preserves a δ^{13} C ratio of -34.31 to -12.07.

ACKNOWLEDGMENTS

I would like to express thanks to the many people who have contributed their help and guidance for this project. Thank you to Dr. Russell Shapiro for his much appreciated guidance, insight and encouragement for this project. I would also like to thank all other faculty members of the Gustavus Geology Department for their suggestions and comments. I also want to extend great thanks to NSF-Biogeosciences for funding and owners of Hanna Ranch for access on their land. Thank you to all other members of the Seep Habitat Investigation Team including Dr. Timothy Lyons, Dr. Karla Persons-Hubbard, Val Morgan, Robin Dahl, Rebecca Rudolph, Hillary Close, Ben Gill, Kristin Hepper, and John Vorhies for your help and comments in the field. Special thanks to Eleanor Bash for her support and contributions throughout this project as well as Brian Goldner for his help in both the field and lab. I greatly appreciate the assistance throughout this project with out you this would not have been possible.

TABLE OF CONTENTS

LIST OF FIGURES AND TABLES

Figures Pages

Tables Pages

INTRODUTION

Methane-seeps are typical features of continental margins, cases where life thrives in a cold and lightless deep-sea ecosystem. Modern seeps occur in a variety of marine tectonic settings (Campbell, 2002) where faulting allows for the release of methane in deeply buried deposits to seep upward to the ocean floor. Modern hydrocarbon seep environments are unique sites that sustain a dense and diverse chemosymbiotic community (Campbell, 2002). Without light for photosynthesis, bacteria and archaea engage in chemosynthesis, the process by which microbes create energy by mediating chemical reactions. The chemosynthetic microbes provide the foundation for vent colonization. The microbes live on or below the seafloor and within the bodies of other vent fauna as symbionts. The dense and diverse invertebrate fauna that live around the seep environment thrive from the seeping fluids in contrast to the sparse distribution of fauna outside of the vent area.

Due to the difficulty of direct observation and recency of their discovery, there is much more to learn about these systems. The evolutionary trends of these systems have drawn much attention from exobiologists who study Earth's extreme environments and whose goal it is to determine ways of recognizing life signatures on other worlds different from the communities seen on Earth (National Aeronautics and Space Administration, 2001).

Ancient hydrocarbon seep and hydrothermal vent deposits have been found in the rock record from the Early Archaean into the Quaternary Period (Campbell, 2002; Peckmann *et al.*, 1999). Seep-carbonates in particular have been recognized in the rock record as early as the Devonian (Goedert *et al.*, 2000). The series of features used to

identify ancient seep deposits include structural and stratigraphic associations as well as distinct mineralogical, geochemical and paleontological features (Campbell, 2002; Shapiro, 2002). Studying the petrographic fabrics, and paragenetic sequence of cement and mineral phases specifically, provides a spatial and temporal framework. This can then be used to address if the seep fluids were venting simultaneously with organism activity. Isotopic geochemical data of individual petrofabrics can be used to trace the changes in the fluid diagenetic pathways of the entire system (Campbell, 2002)

The Tepee Buttes in Colorado are excellent examples of ancient, submarine, hydrocarbon seep deposits. They are Cretaceous in age bridging the gap between modern deposits and very ancient analogues (Shapiro, 2002) as well as adding to the rather sparse record of Mesozoic seep deposits (Peckmann, 2004). By understanding the paleontology of the buttes, as well as the complex petrographic fabrics, we can develop proxies for recognizing ancient methane-driven carbonates in the rock record and aid exobiologists in the search for an extraterrestrial fossil record (Shapiro, 2004).

Geographic Setting

The main Tepee Buttes study area encompasses an area of 4.5 km^2 near Colorado Springs, Colorado (Fig. 1). Similar structures are found across the Cretaceous Interior Seaway from the Texas-Mexico boarder in Ojinaga Formation, Colorado and into the Northern Black Hills of South Dakota spanning an area of 640,000km^2 (Metz, 2000). The Western Interior Cretaceous Basin covered the central region of North America and lined the eastern front of the Ancestral Rocky Mountains (Fig. 2).

Geological Setting

The buttes are a series of conical hills of limestone within the Upper Cretaceous marine Pierre Shale (Fig. 3a). Each butte can reach a height of 10 m and width of 60 m (Kauffman *et al.*, 1996). They are between 76.65 and 75.4 Ma, ranging through four ammonite zones (Howe, 1987). During this time, the Western Interior Cretaceous basin covered central North America. The basin was undergoing periods of widespread and intensive cold seep activity due to early uplift from the Laramide Orogeny (Metz, 2000). Uplift began in the southern region of Colorado and New Mexico and moved north toward South Dakota (Tweto, 1973).

The buttes align in linear rows from Colorado Springs to Boone, Colorado. Individual rows include up to one hundred buttes (Metz, 2000). These structural trends suggest that the seeps were orientated along planes of weakness in the shale recording the northwest trending basement faults of the Laramide Orogeny (Metz, 2000). These faults provided the pathways for methane-rich fluids from the underlying Pierre Shale and Niobrara formations to escape up to the sea floor and support a seep community (Howe, 1987, Fig. 4). The seep habitat supports a number of diverse invertebrate fauna in contrast to the depauperate Pierre Shale (Howe, 1987). Fauna zones in relation to the buttes are used for mapping different environments within ancient seep communities. The macrofauna within the system are dominated by mollusks, with the chemosynthetic lucinid clam *Nymphalucina occidentalis.* Ammonoids, inoceramids and gastropods are also recognized (Howe, 1987).

Previous Work

Gilbert and Gulliver (1885) were the first to study the limestone mounds in the Pierre Shale. They named them the Tepee Buttes due to their shape and resemblance to plains Indians' dwellings within the last century (Howe, 1987). Previous hypotheses of the geological origin of the Tepee Buttes, such as shale hills capped by concretions have been disproved after further study. Alternative hypothesis included that the mounds were formed from carbonate cemented lucinid bivalves (Gilbert and Gulliver, 1895). However, the clams do not colonize the shelly substrates (Kauffman *et al.,* 1996). A third hypothesis is that the buttes were carbonate mud mounds within marine grass beds. However, there has been no vegetally produced carbonate grains or chlorophytes found within the buttes. The hypothesis that remains is that the buttes are sites of submarine seeps inhabited by a diverse community of invertebrates (Kauffman *et al.*, 1996).

Previous lithological studies of the Tepee Buttes have found several distinct lithologies in and around the seep system (Howe, 1987; Shapiro and Frike, 2002). According to these authors, adjacent to the core is a poorly fossiliferous, vuggy, peloidal micrite. The micrite is surrounded by a dense lucinid coquina of *N. occidentalis.* Brecciated limestone pieces surround the coquinas consisting of large blocks that slumped away from the core. Limestone siderite concretions are found encircling the limestone deposit with other interspersed concretions of the seafloor near and around the buttes (Howe, 1987, Fig. 5).

Previous petrographic studies of the Tepee Buttes suggest that the carbonates show evidence for early digenetic cementation (Kauffman *et al.*, 1996). The peloids are not compacted and cements growths is outward from the peloids. Cements consist of

yellow calcite and radial fibrous calcite in botroyiod fans suggesting a submarine seep environment (Kaufman *et al.*, 1996; Savard *et al.*, 1996; Peckmann *et al.*, 2001). Previous studies of work from a variety of methane-seep deposits around the world have also determined that authigenic, microcrystalline carbonates are the dominant phases in the deposit with micrite being the most common variety (Peckmann, 2004). Complex fabrics in the seep system are produced by rapid oxidation and reduction changes with common dissolution horizons (Shapiro, 2002). Dominant grains are peloids and probably microbial in origin (Chafetz, 1986).

Previous geochemical work on the Tepee Buttes includes carbon and oxygen isotope data. $\delta^{18}O$ values range from –1 to –3‰ suggesting normal marine temperatures of 15-25 °C (Kauffman *et al.*, 1996). $\delta^{13}C$ values are extremely depleted from –40 to –45‰ possibly by deriving dissolved carbon from biologic methane oxidation (Kauffman *et al.*, 1996).

METHODS

Field Methods

In the field, 106 buttes were mapped near Colorado Springs and Boone, Colorado with a hand held differential GPS receiver. Outcrop lithofacies were described. Five distinct lithofacies were identified and mapped individually on each butte to create a surficial geologic map identifying lithofacies patterns. Lithofacies recognized in the field were as follows: (I) vuggy limestone with thick cement rinds and coarse calcite spar, (II) packstone dominated by articulated lucinids with vugs and cement rinds, (III) lucinid clams in a packstone with few cements, (IV) limestone concretions found at carbonate and shale interface, (V) microbialite facies mottled dark brown to purple color with little to no fossil material or cement rinds. Rock samples were collected from each lithofacies

on the buttes to analyze if the petrographic fabrics found under the microscope correlate with the lithofacies identified in the field.

Lab Methods

Standard and polished thin sections were made and examined through plane-polarized and cross-polarized light under 40X , 100X and 200X magnification, and under Cathodoluminescence (CL). Oversized thin sections, 5.1 x 7.6 cm, were used for larger samples. Thin sections were finished to 30 microns thick with a polish suitable for the high temperature of the CL microscopy. The Relion Cathodoluminescence system was used to identify the temporal and spatial relationships more accurately. Settings were between 40-60 mTorr, 0.5-1 DCmA and 3.8-5 kV. The luminescence in the CL microscope reveals trace amounts of impurities at several ppm. The calcium in the carbonate rocks is substituted by manganese at several ppm. It is this presence of Mn that causes the flare seen in the CL microscope. Photomicroscopy was used with a Nikon Digital Coolpix 4500 camera connected to the microscope and viewed through a television via a cable. Photomicrographs were taken at fine resolution, 1600 x 1200 pixels. Photos were taken of the different carbonate seep fabrics and entered into a File Maker Pro 6.0 database recording parameters and positions using an *x-y* coordinate system.

RESULTS

Petrofabric data from the Tepee Buttes agree with the petrofabric data found in previous hydrocarbon seep studies (Kauffman *et al.*, 1996; Savard *et al.*,1996; Campbell *et al.*, 2002; Shapiro, 2002; Shapiro and Fricke, 2002; Chafetz, 1986). Analysis reveled carbonates dominated by peloidal grains. Yellow calcite, radial fibrous botryoids and

blocky spar dominated the cement stages. The Tepee Buttes carbonate consists of eight distinct petrofabrics and four erosional events (Table 1). The petrofabrics and erosional events occurred during different times creating a series of paragenetic to diagenetic features. Features were identified under the microscope based on cross-cutting relationships and used to determine the rock's origin and burial history.

Carbonate Phases

Micrite

The earliest petrofabric seen in the Tepee Buttes is a dark-gray to brown micrite, <0.4mm (Fig. 6A). This micrite contains fine siliciclastic (2%) and sulfide material (5%). It is relatively unfossiliferous except for sparse foraminifera and areas of abundant sponge spicules. The micrite exists in the form of intraclasts within an intrapelmicrite or intrapelsparite. The micrite phase is also existent in the form of concretions found in and around the buttes. Under CL, two micrites phases can be distinguished one nonluminesent and the other dark orange. Under the petrographic microscope these two phases are indistinguishable (Fig. 9A).

Pelmicrite

The presence of dark brown peloids in micrite matrix reveals a second carbonate fabric, pelmicrite (Fig. 6B). Two distinct peloids populations are found occurring together. The larger peloids are likely bivalve? fecal pellets with a size ranging from 0.5-1mm along the longest axis of the peloid. The smaller peloids are related to the decomposition of bacterial mats with a size range of 0.05-0.15mm (Fig. 8). The pelmicrite consist of gray-brown micrite with fine siliciclastic (5%) and sulfide materials

(1%). This fabric is relatively unfossiliferous with the exception of sparse foraminifera. Under the CL, the pelmicrite is homogeneous to a mottled dull and dark orange (Fig. 9B).

Intrapelsparite

The intrapelsparite phase consists of intraclasts of micrite and pelmirite (0.1-3.25mm), peloids (0.05-1mm), and spar (0.1-0.5mm). The peloids and intraclasts are cemented by spar radiating from the intraclasts and peloids (Fig. 6C). Shell fragments in the intrapelsparite consist mostly of lucinid clams with a sparitized shell filled with geopetal micrite in the cavity of the lucinid. Foraminifera and inoceramids are also seen in thin section. Under the CL, the intrapelsparite is a bright orange to dark orange color. There are several areas of bright orange color banding around the grains suggesting later digenesis (Fig. 9C).

Intrapelmicrite

Intrapelmicrite contains intraclasts that are slightly larger than the intrapelsparite (0.1-3.25mm). The peloids remain consistant in size (0.05-1mm). The intrapelmicrite has a micrite cement around the intraclasts, peloids and shell fagments rather than spar as in intrapelsparite (Fig. 6D). Intrapelmicrite contains very little sulfide and siliciclastic material (<1%). Cements in the intrapelmicrite include yellow calcite and radial fibrous botryoids (Fig. 10). Fossil fragments of the intrapelmicrite include foraminifera, inoceramids and bivalves. Under the CL, this fabric is a mottled nonluminesent to dark homogenous orange color (Fig. 9D).

Cements

Yellow Calcite

Yellow calcite cement is found surrounding peloids, intraclasts, and micrite as well as interlayered within the botryoids (Fig. 6E). Radial yellow cement bands range from 0.1 to 2 mm thick. Under the CL, this cement appears to be a homogenous dull to bright orange (Fig. 9E).

Radial Fibrous Calcite

The radial fibrous calcite is gray to tan, forming in radiating botryoids emerging from the yellow cement (Fig. 6F). The botryoids have undulose extinction that is in optical continuity with the later spar crystals (Fig. 11). There are banding patterns in the botryoids from light tan to dark gray from inclusions and corrosion bands. Botryoids range in size from 0.3 to 1.25 mm diameter. Clear and distinct banding patterns are seen under the CL from bright orange to dark orange (Fig. 9F).

Spar

The calcite spar 1 is a clear blocky pore filling cement (Fig. 6G). It has subhedral to euhedral crystals, range from 0.25 to 1mm across. Under the CL, it appears nonluminesent to dark orange (Fig. 9G). Spar 1 is found replacing parts of the early micrite and botryoidal fabrics in a process called sparitization. The second calcite spar (Spar 2) is also a clear and blocky calcite, but fills in later fractures in the carbonates (Fig. 6H). Spar crystals are slightly larger from spar 1 (0.3 to 1 mm). Under the CL, spar 2 appears nonluminesent to dark orange (Fig. 9H).

Erosional Events

Petrofabric analysis reveals four erosional events throughout the paragenetic to diagenetic sequence. These consist of two common sulfide phases (EE1, EE3) and two erosional events (EE2, EE4). Erosional event one (EE1) postdates micrite and pelmicrite deposition. It is characteristic of dark sulfide-rich corrosive nodules (Fig. 7A). Erosional event two (EE2) postdates EE1 and is characteristic of an erosional surface that can be seen eroding through the sulfide phase. Deposition and cementation of intrapelsparite and intrapelmicrite occurred after EE2 filling in the eroded vugs. This surface was then later corroded by another sulfide phase, erosional event three (EE3, Fig. 7B). Cementation of yellow calcite and radial fibrous botryoids postdate EE3. Botryoids can be seen to have an erosional surface on several edges where crystal fans have been broken before spar 1 filled in the void space, representing erosional event four (EE4, Fig. 7C).

Lithofacies

Petrofabrics were analyzed within each lithofacies to find any correlations between fabric and facies. Lithofacies 1 consists of abundant vugs with thick cement rinds and coarse calcite spar. Lucinid bivalves are the dominant fauna (Fig. 12A). The carbonate is a mottled gray and brown micrite. Lithofacies II is dominated by articulated lucinids with fewer vugs and cement rinds (Fig. 12B). Lithofacies III is also dominated by lucinid clams in micrite containing many small fractures filled in with spar (Fig. 12C). Lithofacies IV consists of limestone concretions and is found generally in the shale at the carbonate and shale interface (Fig. 12D). Lithofacies V is a microbialite facies

containing little to no fossil material or cement rinds (Fig. 12E). The microbialite is a mottled dark brown to purple color.

A model showing lithofacies arrangement was created based on the distribution of lithofacies that were mapped (Fig. 13). Instead of concentric facies arrangement suggested by previous studies (Kauffmann *et al.*, 1996, Fig. 5) after detailed field mapping of the Tepee Buttes I found there to be no clear pattern in butte development. All lithofacies were found in an unevenly distributed pattern on the buttes with the exception of lithofacies IV which was seen in the shale and limestone interface and not directly related to butte development. Lithofacies III was only found on buttes at a higher elevation suggesting that it is formed at or above the sediment water interface where there could have been more erosion and weathering (Fig. 13). The stratigraphic pattern displays interlayered shale and lucinid coquina layers suggesting vertical accumulation of carbonate and sediment. The present conical shape of the buttes is a relatively new feature due to later erosion of the Pierre Shale around the more resistant carbonate mounds. Evidence from the road cut and Boone, CO shows only horizontal bedding and no conical shape in the butte structure suggesting that during carbonate formation the mounds had a low relief on the sea floor.

Results of the petrofabric and lithofacies analysis are documented in Table 1. The micrite fabric is found in lithofacies I, II, and IV either as a homogeneous matrix or as intraclasts. Pelmicrite is found in lithofacies I, II, and III also either as a homogeneous matrix or as intraclasts. Intrapelmicrite occurs in lithofacies I, II, III, and V. Intrapelsparite also occurs in lithofacies I, II, III, and V as does the intrapelmicrite. All cement fabrics including yellow calcite, botryoids, spar 1 and 2 all occur in lithofacies I,

II, III, and V. These results show that all most every petrofabric occurs in each lithofacies with the exception of only micrite in the concretions, lithofacies IV. Lithofacies I, II, III and IV contain zones of homogeneous micrite. The micrite could be related to later diagenesis or could be original. Lithofacies V contains no micrite, only intrapelsparite and intrapelmicrite and cements.

Further analysis was done to find a general areal percentage of each petrofabric for each lithofacies and these data are summarized in table 2. Lithofacies I contains an even distribution of petrofabrics, but is dominated by botryoids (36%) and intrapelmicrite (32%). The remaining petrofabric percentages for lithofacies I consist of 12% intrapelmicrite, 12% yellow calcite and 7% spar 1. Lithofacies II, III and V are dominated by intrapelsparite. Lithofacies II is comprised of 79% intrapelsparite. The remaining petrofabrics in lithofacies II include yellow calcite (5%), botryoids (5%), micrite (6%) and spar 1 (3%) which also occur in a relatively even distribution of petrofabrics. Lithofaceis III is comprised of 78% intrapelsparite and 22% spar 2 found in the fractured areas. Lithofacies V is dominated by 95% intrapelsparite and 5% spar 1 found in the remaining void spaces. Lithofacies IV is composed entirely of micrite. Intrapelsparite is the most widely occurring petrofabric in each lithofacies. Lithofacies I contains the greatest area of cement phases. Lithofacies II also contains a high area of cement phases compared to lithofacies III, IV or V.

DISCUSSION

A paragenetic and diagenetic sequence was created from analyzing the cross-cutting relationships of the petrofabrics to determine the conditions during early and late

phases of seep development. Micrite 1 represents the original micrite mud (Fig. 6A) and more than one phase is recognized under the CL. There is little original micrite remaining due to early diagenetic processes. The micrite that remains is present in the form of intraclasts and rarely in a homogenous micrite zone. The pelmicrite phase contains original peloids in a micrite mud (Fig. 6B) that were deposited concurrently with the original micrite. The peloids appear as the same color as the micrite matrix under the CL, providing evidence that the cementation of the fabrics was concurrent or evidence for later diagenetic micritization (Fig. 9B). The peloids are hard to distinguish by luminescent characteristics in most areas and appear as a homogeneous micrite.

A sulfur-rich corrosive event (EE1) later eroded the micrite and pelmicrite and is preserved as irregular dark sulfide nodules (Fig. 7A). The presence of the sulfides suggests that carbonate production occurred within the sulfate reduction zone. Following the corrosion there was erosion, (EE2) ripping up clasts of micrite and pelmicrite. These intraclasts were deposited with fragments of shells and make up the intrapelsparite and intrapelmicrite that was deposited after EE2. The grains are not compacted suggesting rapid cementation (Fig. 6G).

The cementation began with anhedral yellow calcite (Fig. 6E) likely formed from replacement of the early micrite due to similar CL patterns (Campbell, 2002). Precipitation of the radial fibrous botryoids after the yellow calcite resulted from alternating redox pulses of methane-rich and sulfate-rich pore fluids, recorded in distinct dark to light banding patterns under the petrographic and CL microscopes (Fig. 9F). Remaining pore spaces were occluded by blocky late stage spar.

Burial sparitization and micritization altered the intrapeloidal fabrics and cements, obscuring original mineral boundaries (Fig. 14). The original cement boundaries and previous fabric patterns can be distinguished under the CL in the sparitized zones (Fig. 9C). However, the micritized zones are homogeneous with little distinction between the grains and their cements (Fig. 9D). Further diagenesis also created fractures within the rock that were later filled in with a late stage clear blocky spar 2 (Fig. 6H).

CONCLUSIONS

Five distinguishable lithofacies are found in the Tepee Buttes carbonates. Within these carbonates there are eight distinct petrofabrics occurring in a consistent paragenetic to diagenetic sequence. Of the eight petrofabrics, there are four main carbonate phases and four cement phases. Two common sulfide phases and two distinct erosional events are also seen within the sequence. This sequence was deduced using crosscutting relationships and gives a temporal and spatial framework for carbonate formation. A similar sequence is also seen in the concurrent studies of other seep carbonates including Californian and Canadian Arctic Mesozoic, suggesting comparative fluid generation and evolution despite their geographically and geologically distinct locations (Campbell, 2002; Beauchamp and Savard, 1992). Like modern seeps, these carbonates most likely formed from geochemical changes brought on by methanotropic bacteria, oxidizing the methane, and sulfate reducing bacteria. Petrographic analysis reveals a consistent pattern of seep cement stratigraphy with generations of precipitation and dissolution representing alternating periods of activity and inactivity of the bacteria. When no methane oxidation, occurs, there is no formation of carbonate and instead dissolution of earlier cements is

likely to occur. Further analysis of the carbon, oxygen and sulfur isotopes of individual petrofabrics within each lithofacies is needed to confirm bacterial activity in the formation of this carbonate and track diagenetic fluids that can't be determined by petrographic and CL microscopy alone. This would provide for a greater understanding of the seep fluids and their pathways in the petrofabrics and possibly correlate to distinct lithofacies to distinguish a pattern of butte development.

REFERENCES CITED

Campbell, K.A. Farmer, J.D. and Des Marais, D., 2002, Ancient Hydrocarbone seeps from the Mesozoic convergent margin of California: Geofluids, 2, p. 63-94.

Chafetz, H.S., 1986, Marine peloids: a product of bacterially induced precipitation of calcite: Journal of Sedimentary Petrology, 56, p. 812-817.

Gilbert, G. K., and Gulliver, F. P., 1895, Tepee Buttes (Colorado): Science, v. 1, p. 59-65.

Goedert, J. L., and Benham S. R., 2003, Biogeochemical processes at ancient methane seeps: The Bear River site in southwestern Washington: Geological Society of America Field Guide, v. 4, p. 201-208.

Goedert, J. L., J. Peckmann, and Reitner, J., 2000, Worm tubes in allochthonous cold seep carbonate from lower Oligocene rocks of western Washington: Journal of Paleontology, 74, p. 992-999.

Howe, B., 1987, Tepee Buttes; a Petrological, Paleontological, Paleoenvironmental Study of Cretaceous Submarine Spring Deposits. [Masters thesis]: Boulder, University of Colorado.

E. G. Kauffman, M. A. Arthur, B. Howe, P. A. Scholleand Howe, B., 1996, Widespread Venting of Methane-Rich Fluids in Late Cretaceous (Campanian) Submarine Springs (Tepee Buttes), Western Interior Seaway, U.S.A.: Boulder Colorado, Geology, 24, p. 799-802.

Metz, C., 2000, Upper Cretaceous (Campaian) Sequence and Biostratigrapy, West Texas to East Central Utah; and Development of Cold seep Mounds in the Western interior Cretaceous Basin. [Ph.D thesis]: Texas A and M University.

Marshall, D. J., Giles, J. H., and Mariano, A., 1990, An Instrument for Cathodoluminescence and Energy Dispersive Spectroscopy: American Laboratory, p. 30-45.

National Aeronautics and Space Administration, 2001, Astrobiology Science Goals. Available at: http://astrobiology.arc.nasa.gav/raodmap/gaols/index.html.

Peckmann, J., Thiel, V., Michaelis, W., Clari, P. Gaillard, C., Martire, L., and Reitner, J., 1999, Cold seep deposits of Beauvoisin (Oxfordian; southeastern France) and Marmorito (iocene; northern Italy): microbial induced authigenic carbonates. International Journal of Earth Science, 88, p. 60-75.

Peckmann, J., Reimer, A., Luth, U., Luth, C., Hansen, B.T., Heinicke, C., Hoefs, J., and Reitner, J., 2001, Methane-derived carbonates and authigenic pyrite form the northwestern Black Sea: Marine Geology, 177, p. 129-150.

Peckmann, J., and Thiel, V., 2004, Carbon cycling at ancient methane seeps: Chemical Geology, 205, p. 443-467.

Savard, M.M., Beauchamp, B. and Veizer, J., 1996, Significance of aragonite cements around the Cretaceous marine methane seeps: Journal of Sediment Res., 66, p. 430-438.

Shapiro, R. S., 2002, Are Proterozoic cap carbonates and isotopic excursions a record of gas hydrate destabilization following Earth's coldest intervals?: Geology, 30, p. 761-762.

Shapiro, R., and Frike, H., 2002, Tepee Buttes: Fossilized methane-seep ecosystems Geological Society of America Annual Meeting Guidebook, Geological Society of America, Boulder, Colorado, p. 94-101.

Shapiro, R. S., 2004, Recognition of fossil prokaryotes in Cretaceous methane seep carbonates: relevance to astrobiology: Astrobiology. v. 4, p. 438-449.

Tweto, O., 1975, Laramide (Late Cretaceous-Early Tertiary) Orogeny in the southern Rocky Mountains: Geological Society of America Memoir, v. 144, p.1-44.

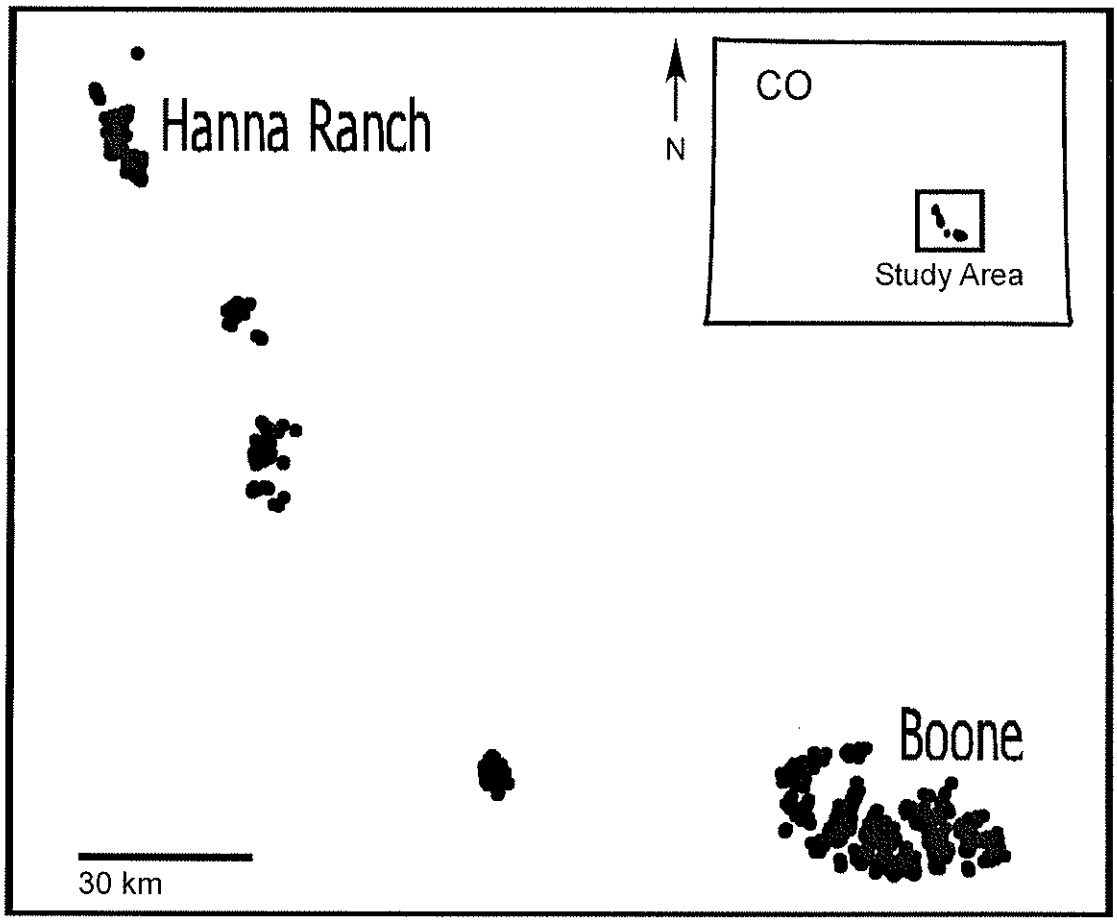

Figure 1. Map of the Tepee Buttes study area in Colorado showing 831 butte at Hanna Ranch and Boone localities. One dot represents one butte.

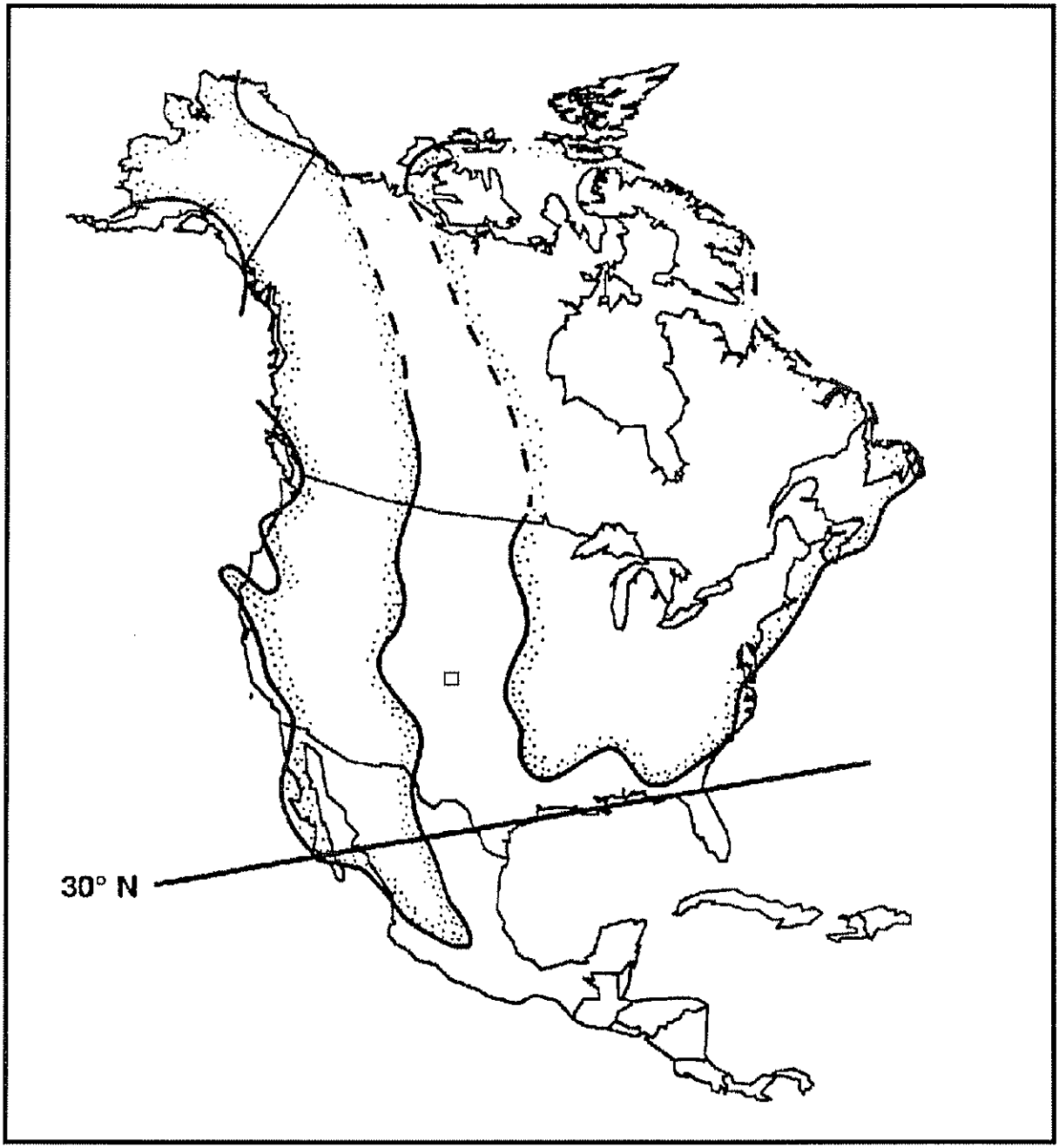

Figure 2. Map of the Western Interior Cretaceous Seaway covering the central region of North America in the late Cretaceous Period. Study area is marked as a box. (Metz, 2000).

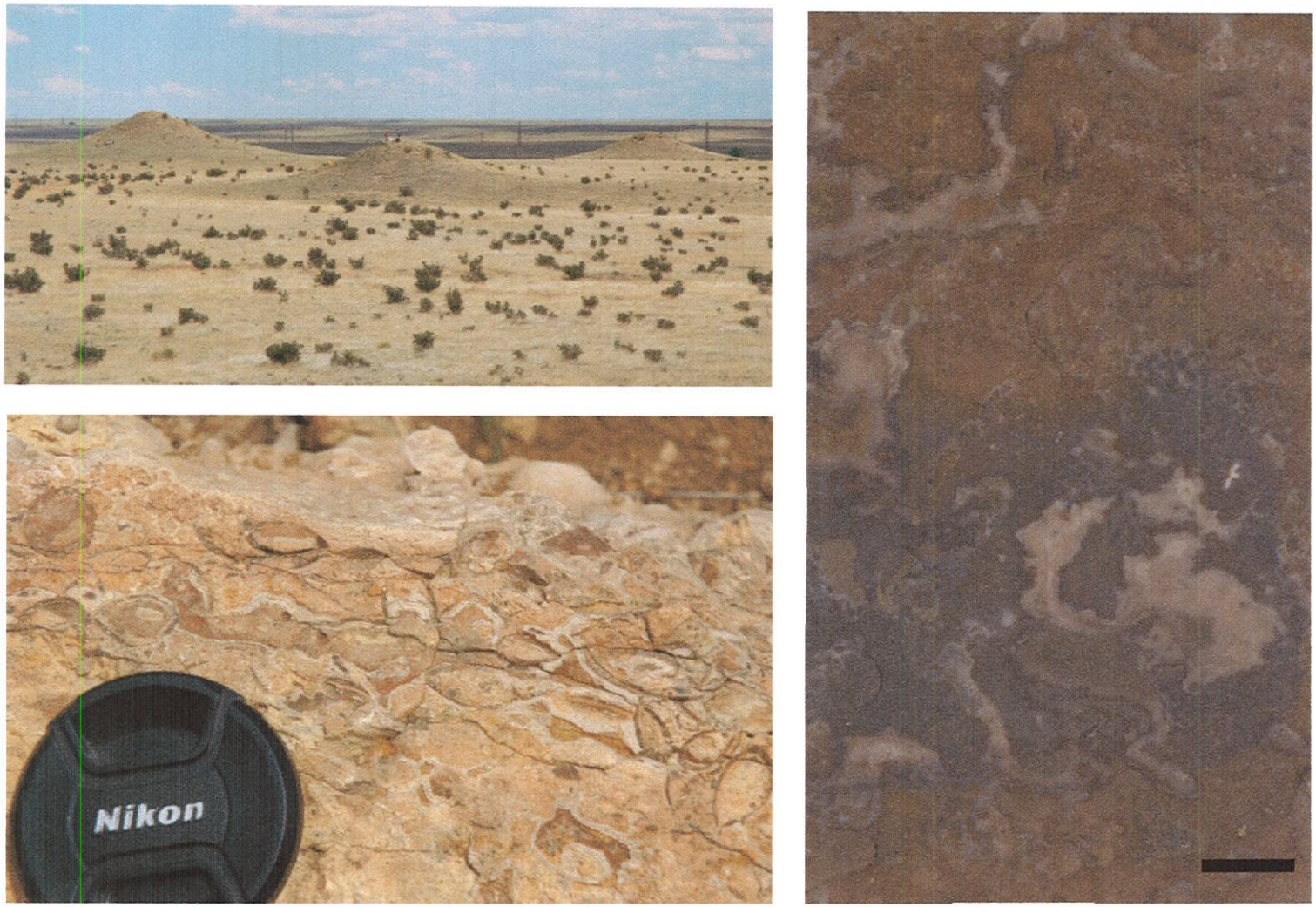

Figure 3. Outcrop, hand sample and petrographic characteristics of the Tepee Buttes Carbonates. (A) Hanna Ranch field locality showing isolated seep mounds. (B) Outcrop block from Boone site showing layered cements and lucinid bivalves. Cap is 7 cm aross for scale (C) Typical thin section view of lithofacies I, showing dark micrite with peloids and light colored calcite cements lining void spaces. Scale bar is 1 cm.

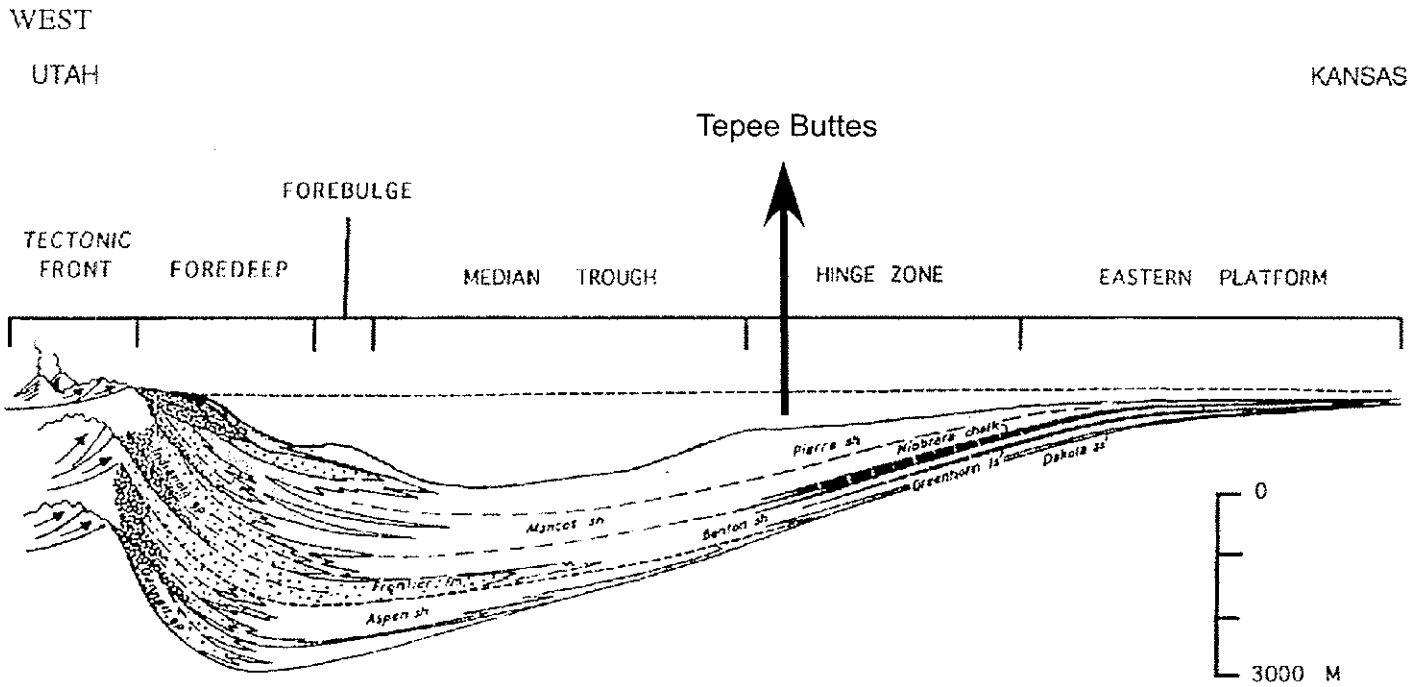

Figure 4. West to east cross section of the Western Interior Seaway showing study area tectonic front, foredeep, forebulg, and backbulg basin (Metz, 2000).

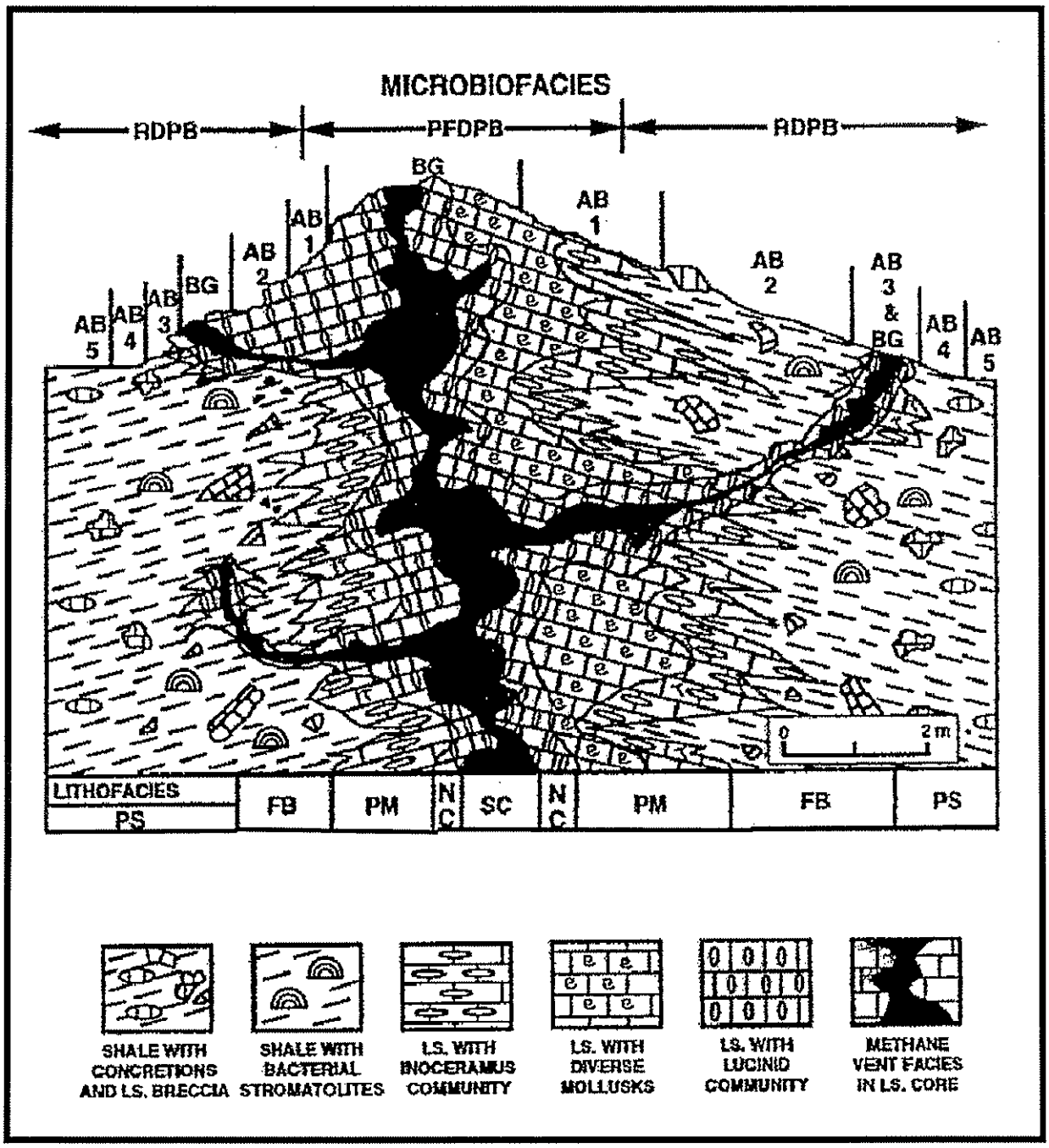

Figure 5. Map showing distribution of lithofacies. Lithofacies: SC-spring core facies, NC-*Nymphalucina* coquina, PM-pelletoid micrite facies, FB-flank brecias, PS-concretionary Pierre Shale (Modified from Kauffman, 1996) Compare to revisions in figure 13.

Table 2. Areal extent of petrographic fabrics for each lithofacies

Lithology	Petrofabric	Areal percentage
I	Intrapelmicrite	32.0
	Intrapelsparite	12.0
	Yellow Calcite	12.2
	Botryoids	36.4
	Spar 1	7.3
II	Intrapelsparite	79.9
	Yellow Calcite	5.4
	Botryoids	5.3
	Micrite	6.2
	Spar 1	3.4
III	Intrapelsparite	78.5
	Spar 2	21.5
IV	micrite	100.0
V	Intrapelsparite	94.7
	Spar 1	5.3

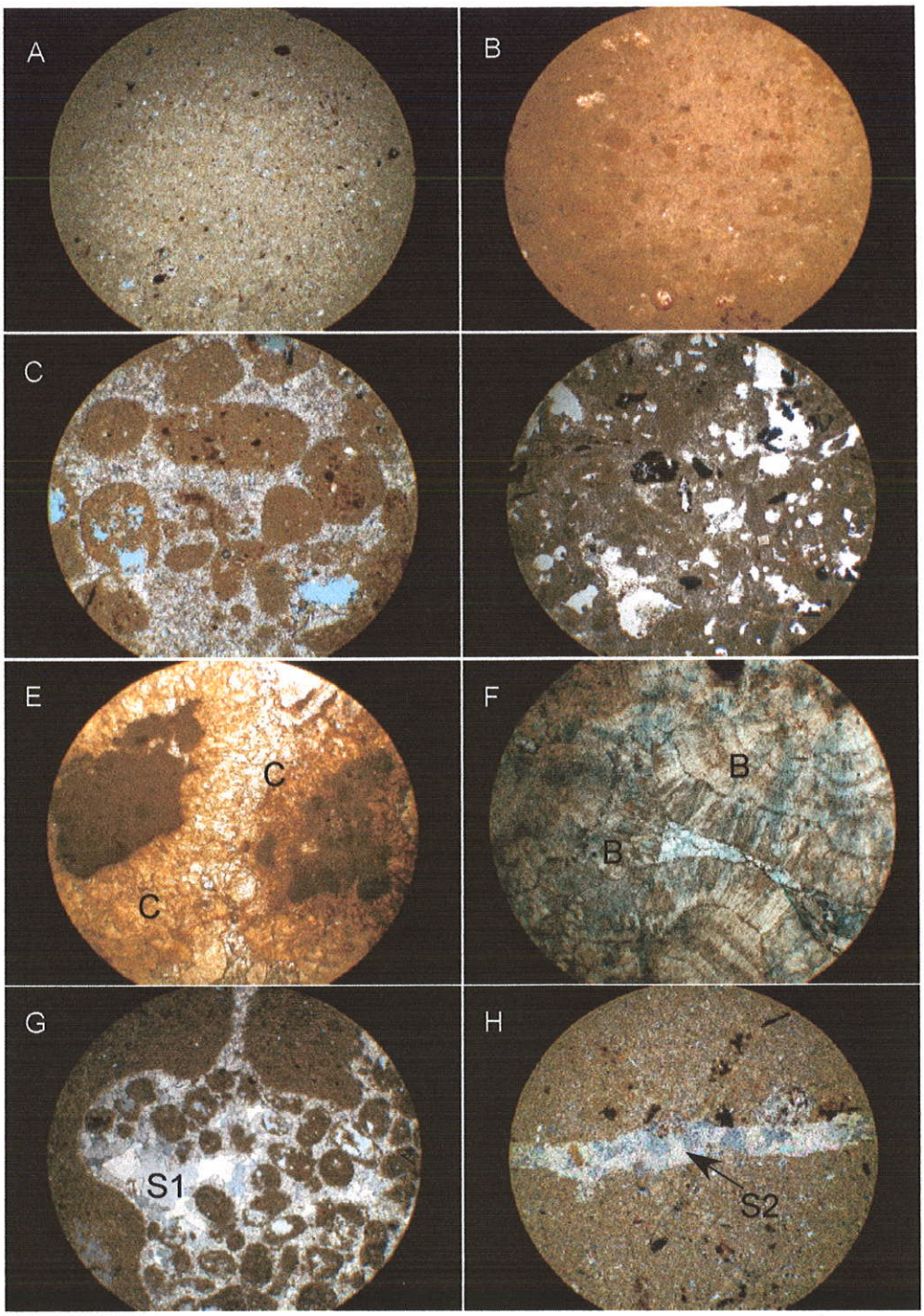

Figure 6. Photomicrographs of all of the petrographic fabrics seen in the Tepee Buttes. Each photomicrograph was taken at 40X under cross polars. Diameter of the view for each photomicrograph is 4.5 mm (A) Micrite. (B) Pelmicrite. (C) Intrapelsparite. (D) Intrapelmicrite. (E) Yellow Calcite shown as C. (F) Radial fibrous botryoidal calcite shown as B. (G) Spar 1 shown as S1. (H) Spar 2 shown as S2.

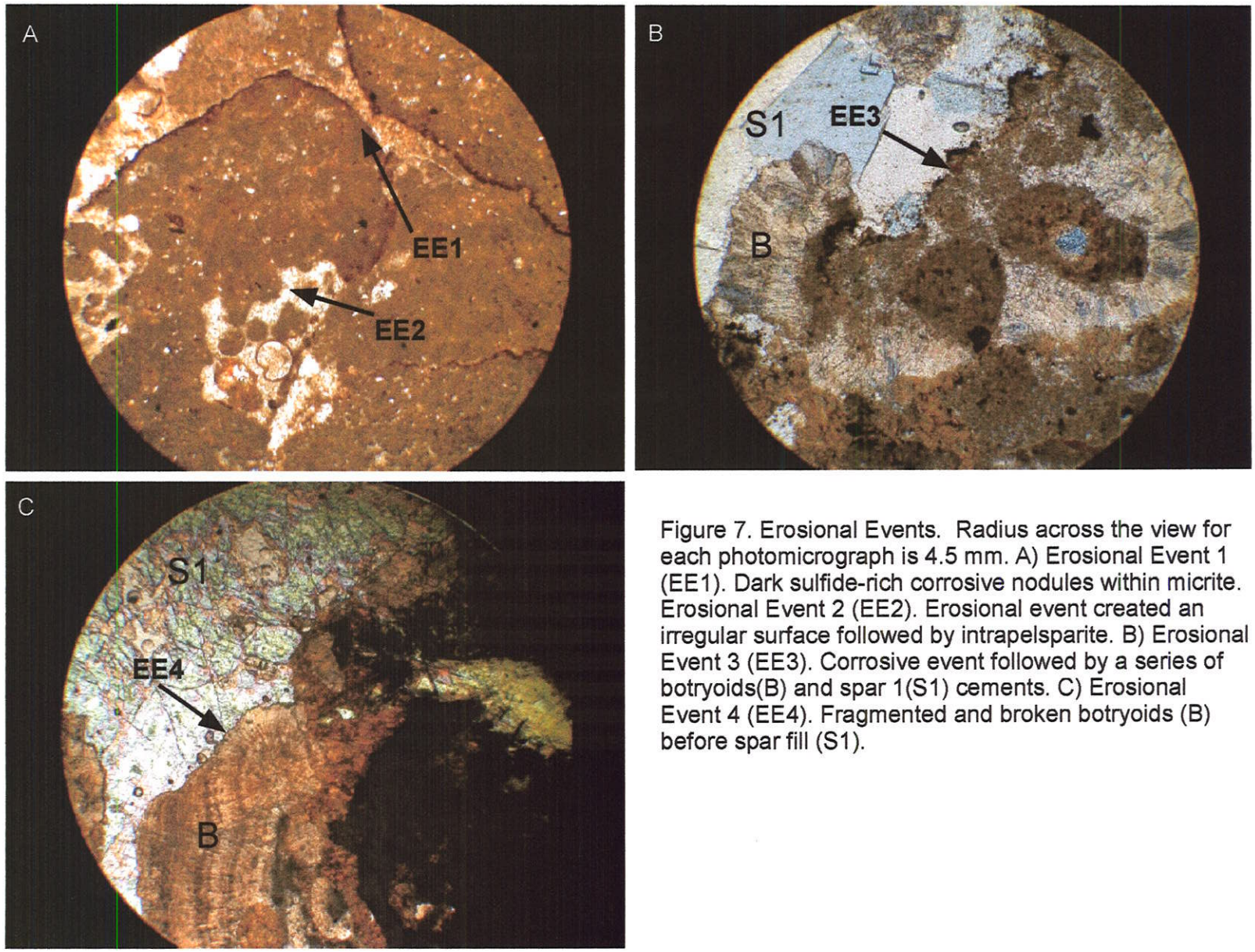

Figure 7. Erosional Events. Radius across the view for each photomicrograph is 4.5 mm. A) Erosional Event 1 (EE1). Dark sulfide-rich corrosive nodules within micrite. Erosional Event 2 (EE2). Erosional event created an irregular surface followed by intrapelsparite. B) Erosional Event 3 (EE3). Corrosive event followed by a series of botryoids(B) and spar 1(S1) cements. C) Erosional Event 4 (EE4). Fragmented and broken botryoids (B) before spar fill (S1).

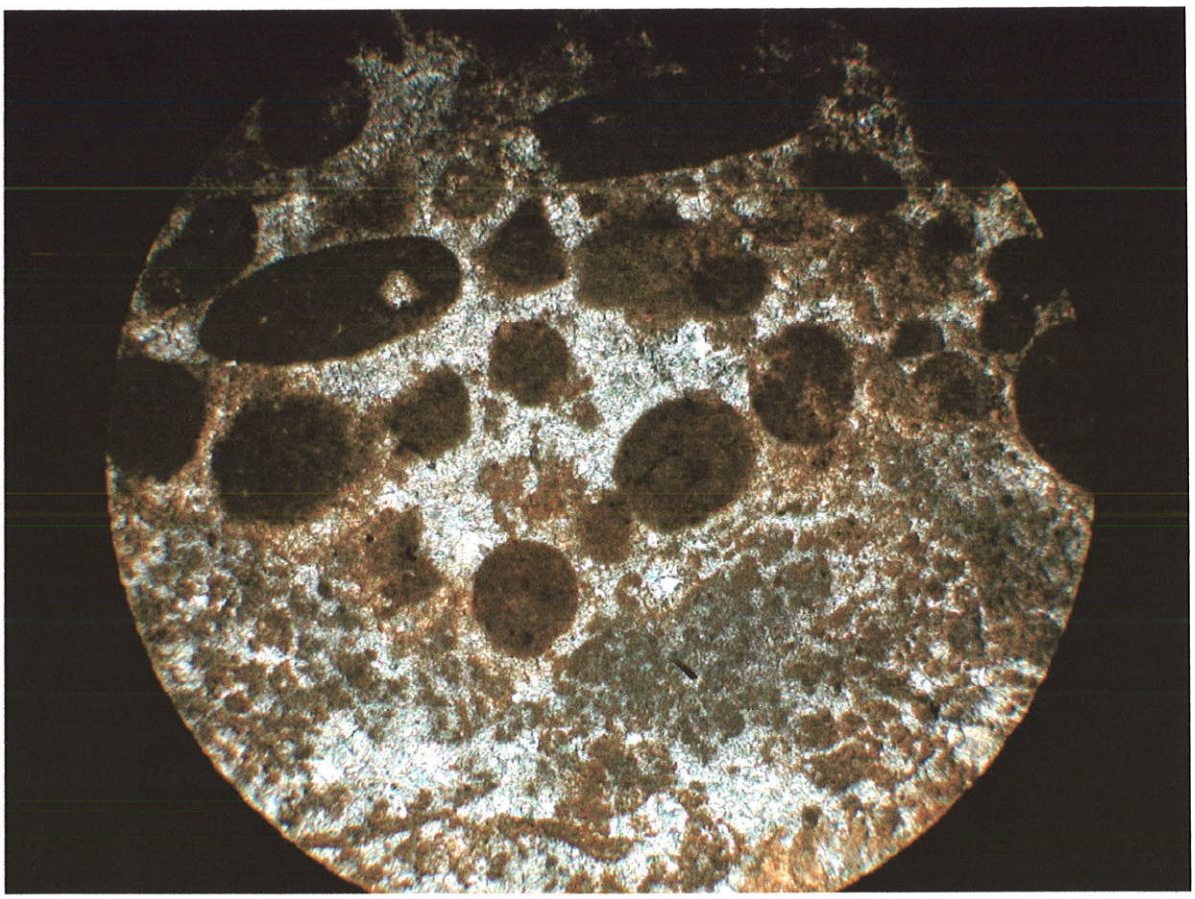

Figure 8. Two distinct sizes of peloids found in the Tepee Buttes (A) is from degrading microbial mats (0.05-0.15mm) and (B) is from fecal pellets (0.5-1mm). The diameter of the view is 4.5mm.

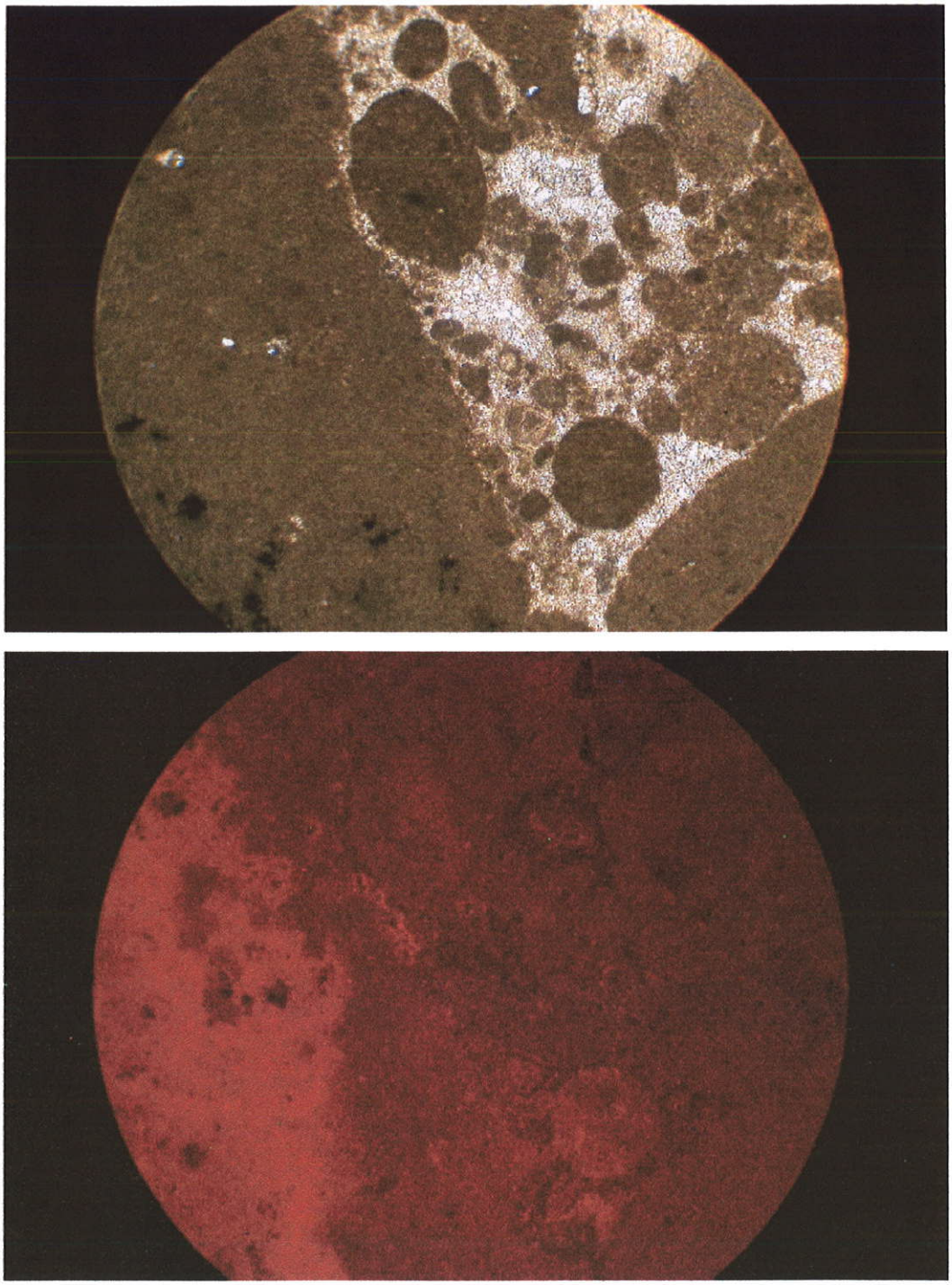

Figure 9A. Micrite. Diameter of circle is 4.5mm. A) Photomicrograph of micrite under the petrographic microscope B) Photomicrograph of the same view under the CL microscope showing two distinct micrites.

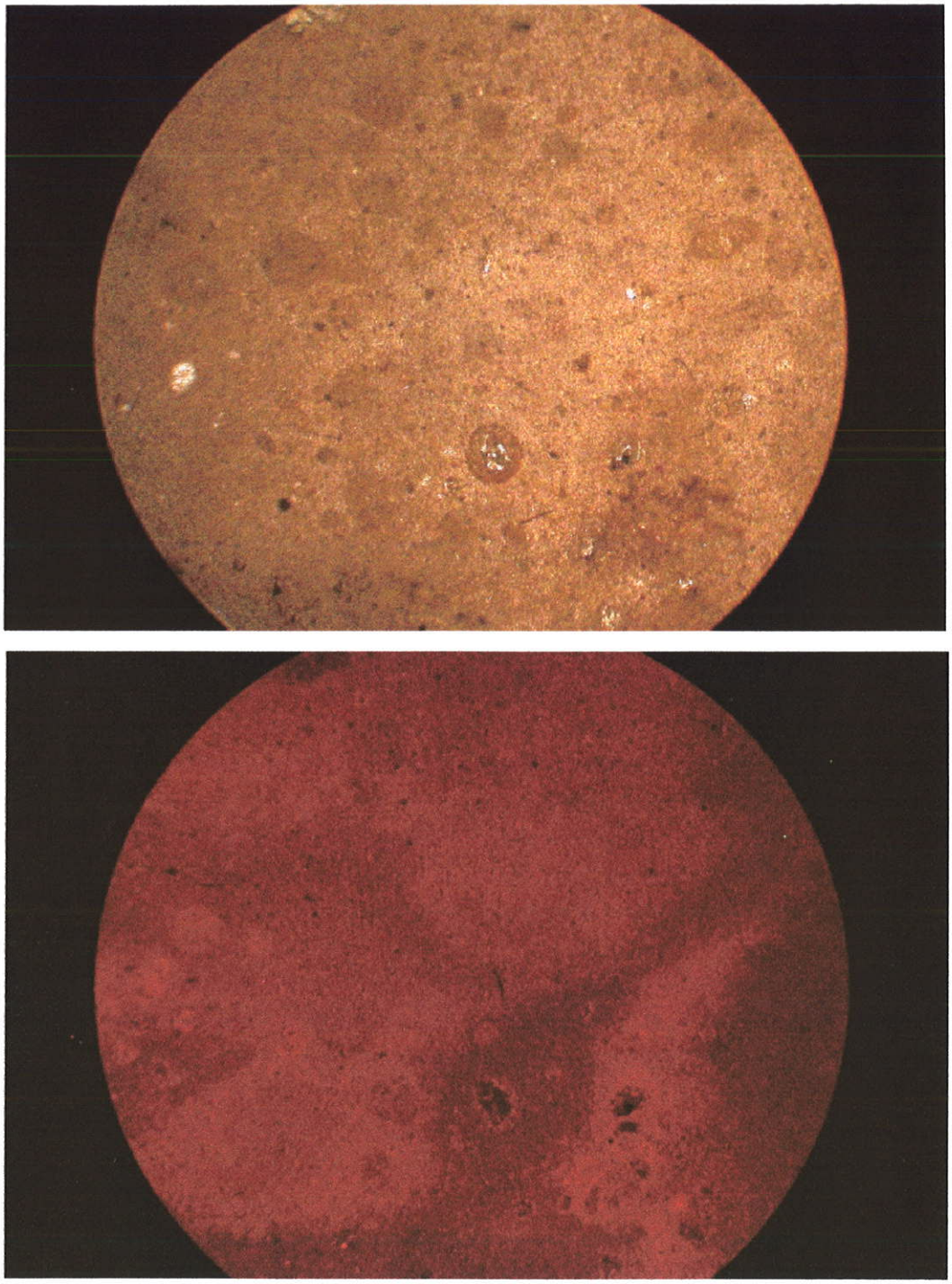

Figure 9B. Pelmicrite. Diameter of view is 4.5mm. A) Photomicrograph of pelmicrite under the petrographic microscope B) Photomicrograph of the same view under the CL microscope.

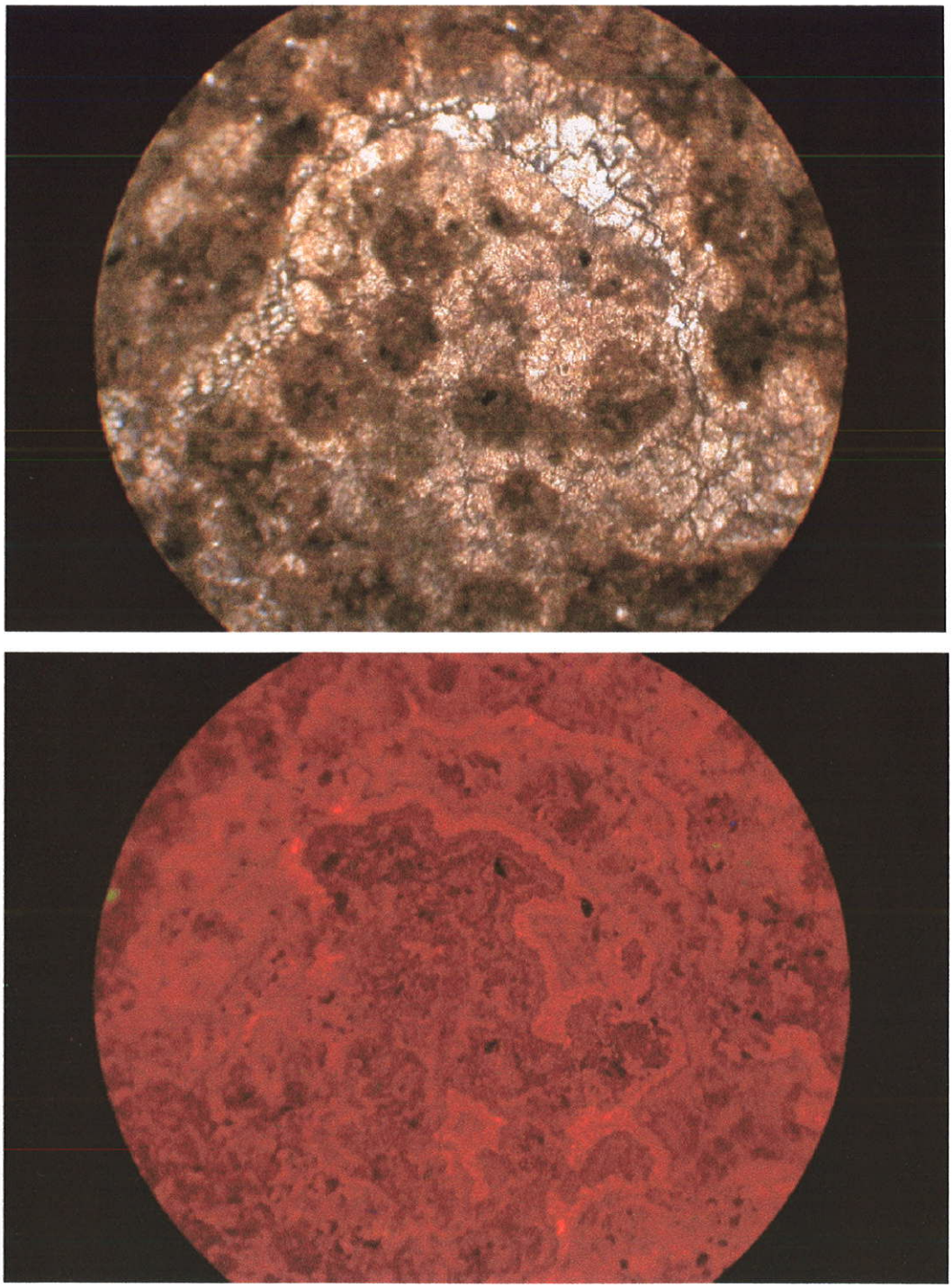

Figure 9C. Intrapelsparite. A)Photomicrograph of intrapelsparite under the petrographic microscope B) Photomicrograph of the same view under the CL microscope.

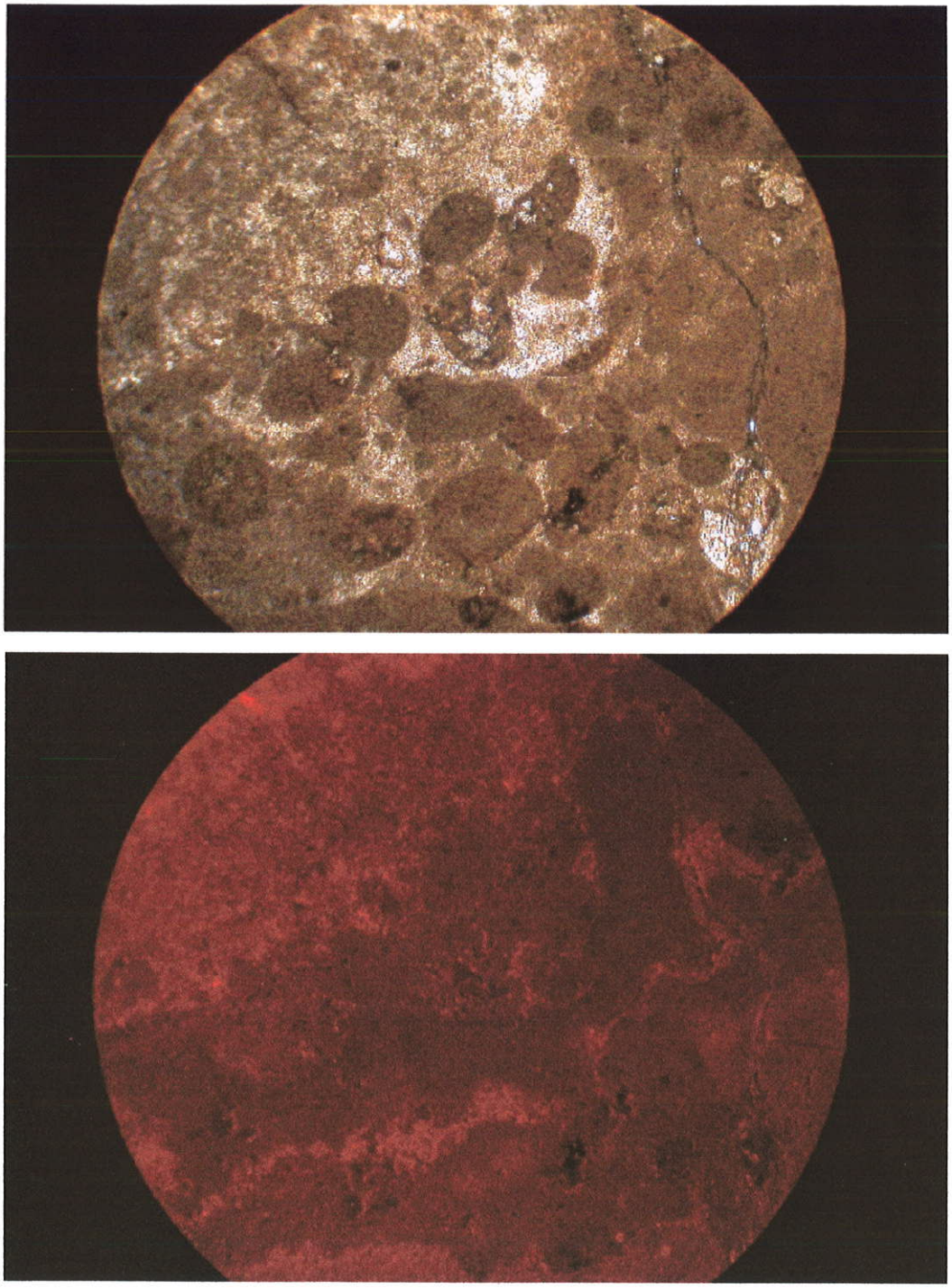

Figure 9D. Intrapelmicrite. A) Photomicrograph of intrapelmicrite under the petrographic microscope B) Photomicrograph of the same view under the CL microscope.

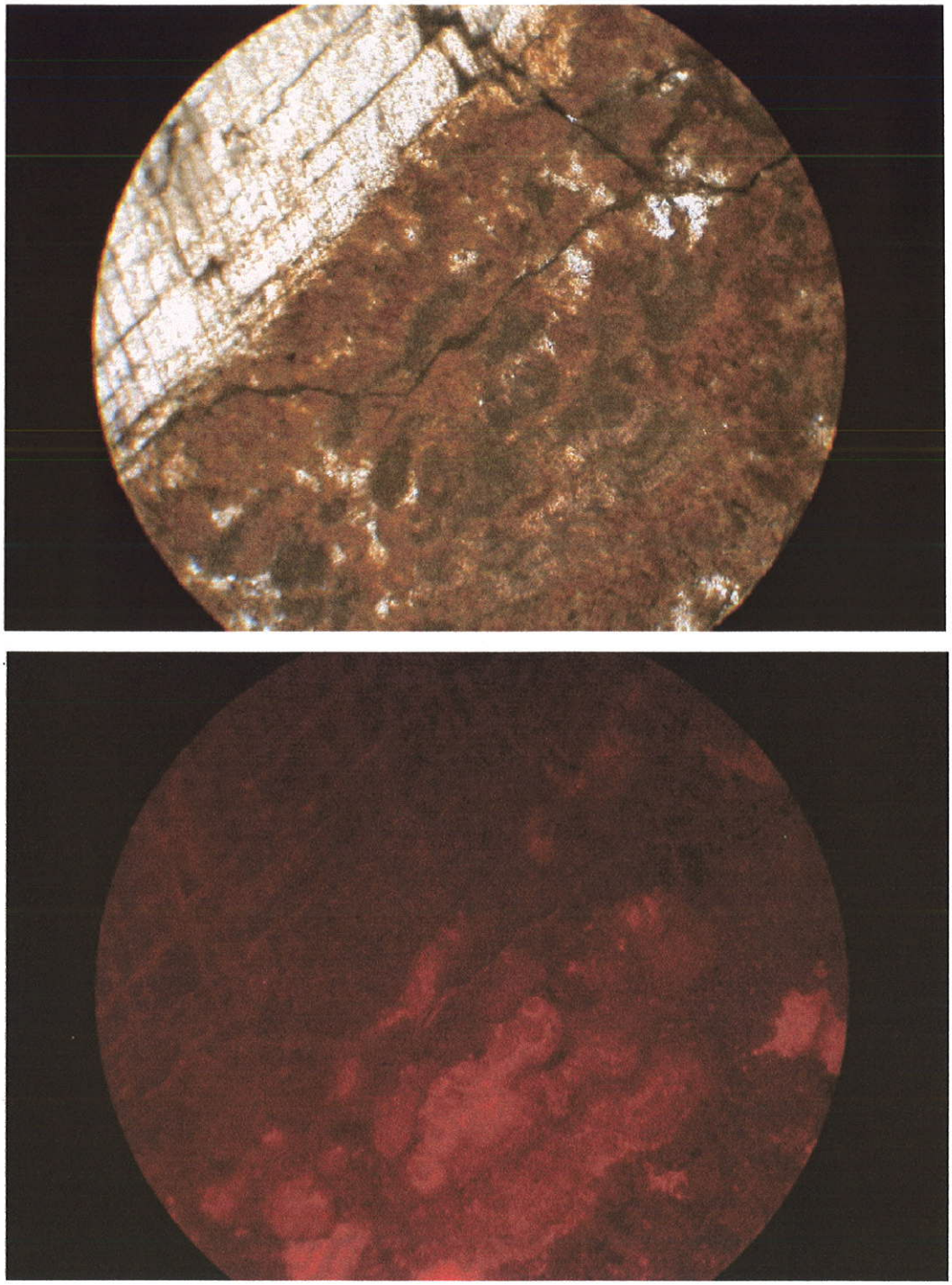

Figure 9E. Yellow Calcite. Diameter of view is 4.5mm. A) Photomicrograph of yellow calcite cement under the petrographic microscope B) Photomicrograph of the same view under the CL microscope.

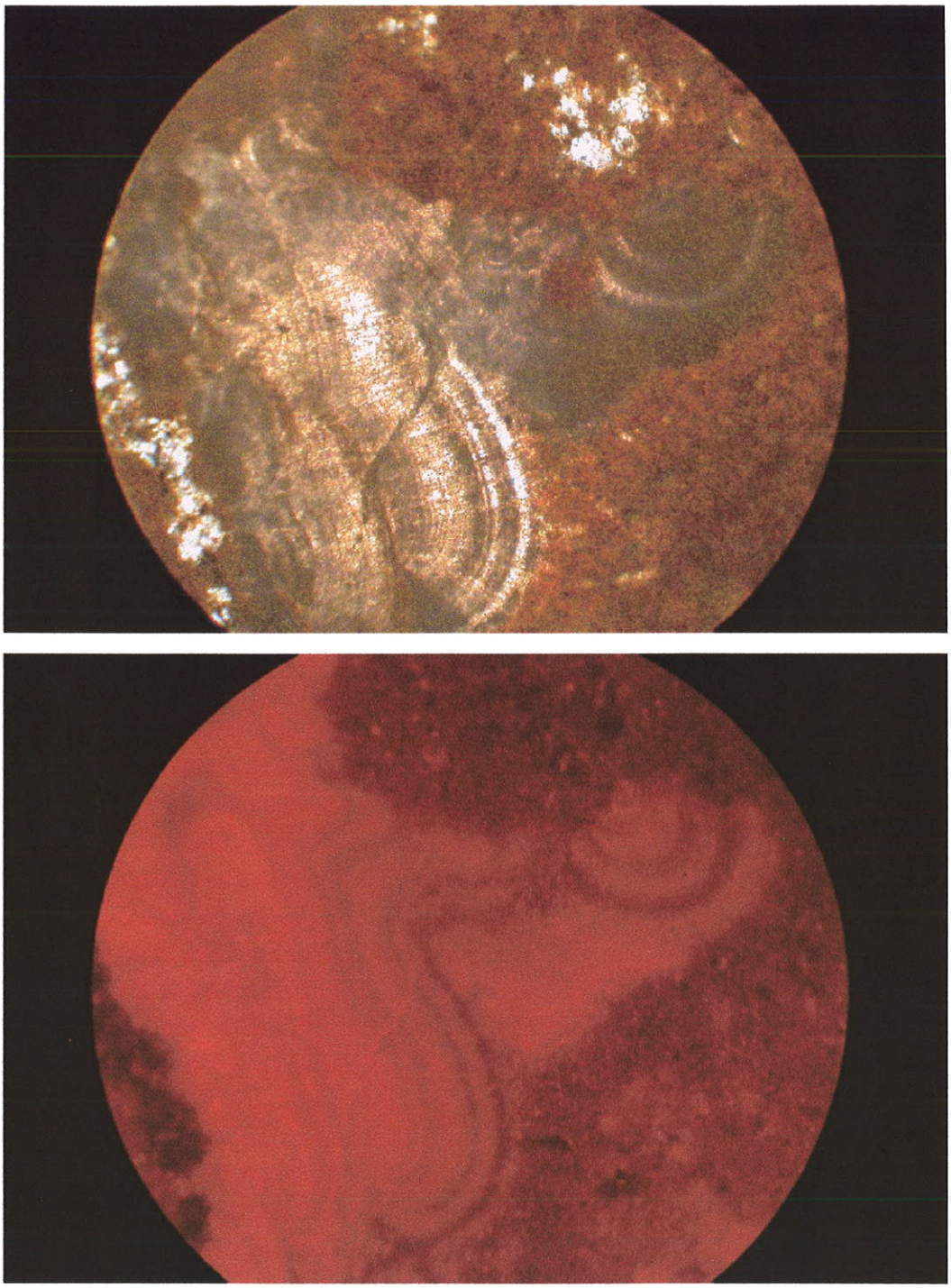

Figure 9F. Radial fibrous calcite cement. Diameter of view is 4.5mm.
A) Photomicrograph of radial fibrous calcite cement under the petrographic microscope B) Photomicrograph of the same view under the CL microscope.

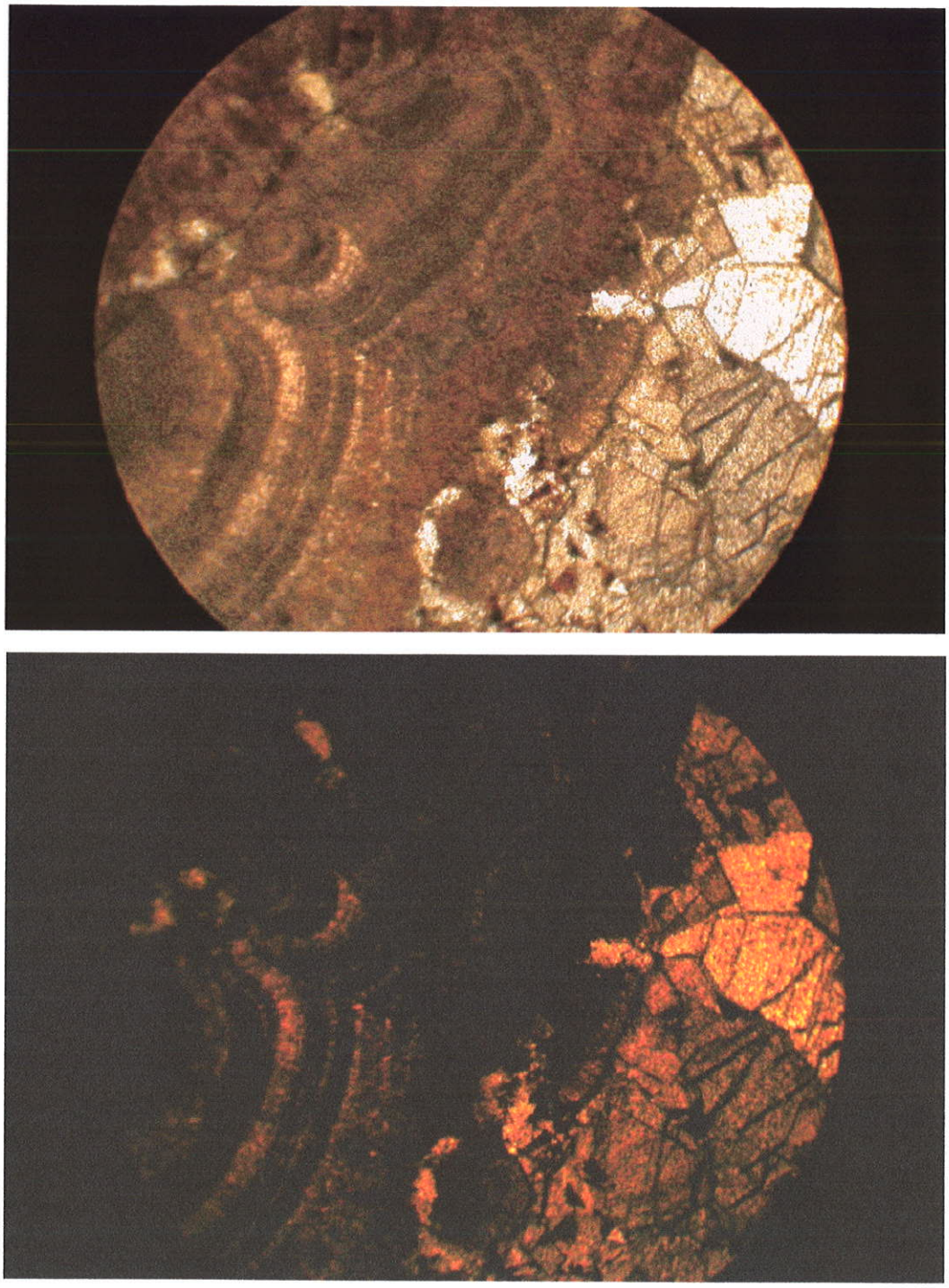

Figure 9G. Spar 1. Diameter of view is 4.5mm. A) Photomicrograph of spar 1 cement under the petrographic microscope. B) Photomicrograph of the same view under the CL microscope.

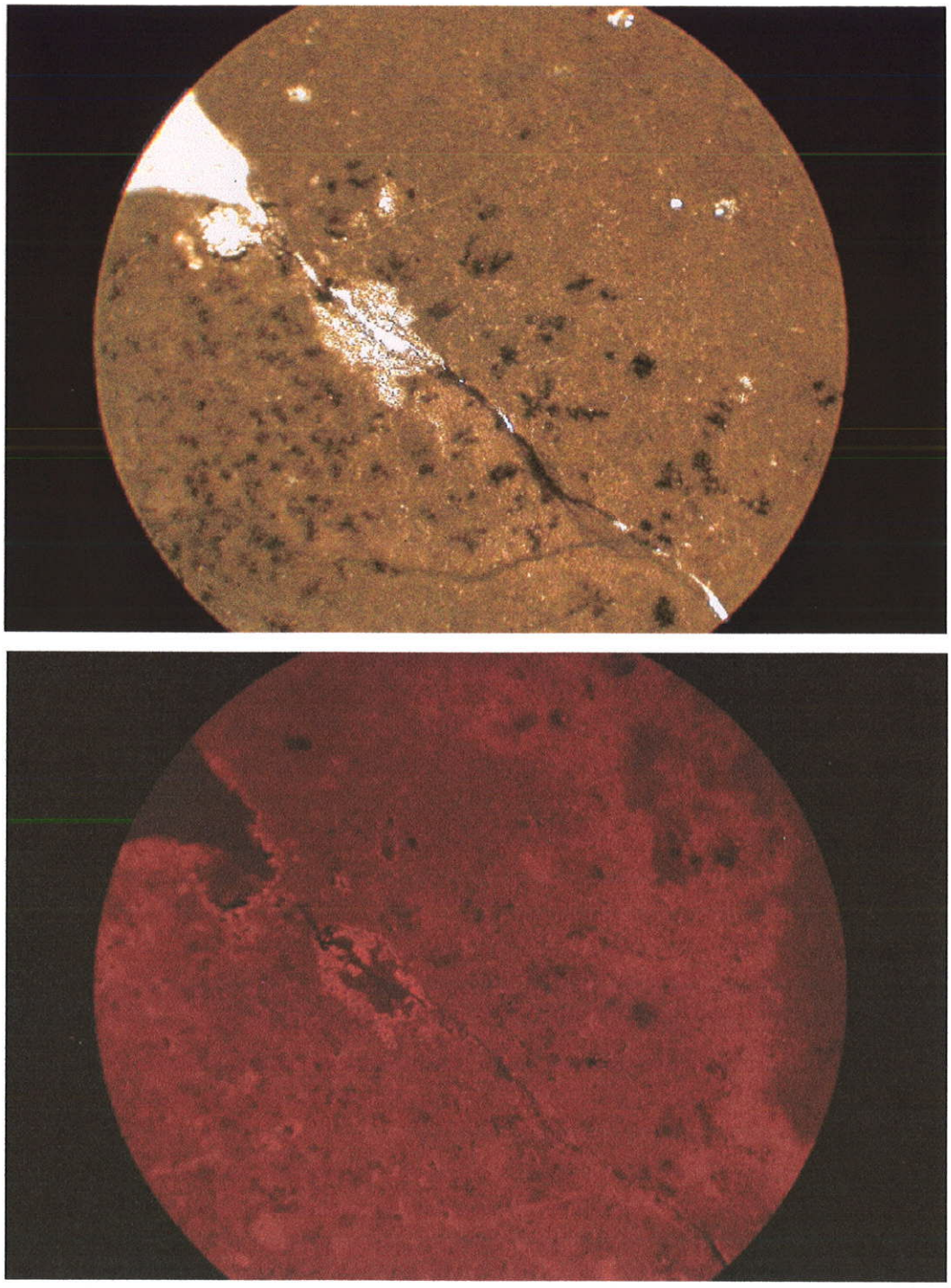

Figure 9H. Spar 2. Diameter of view is 4.5mm. A) Photomicrograph of spar 2 cement under the petrographic microscope B) Photomicrograph of the same spar 2 cement under the CL microscope.

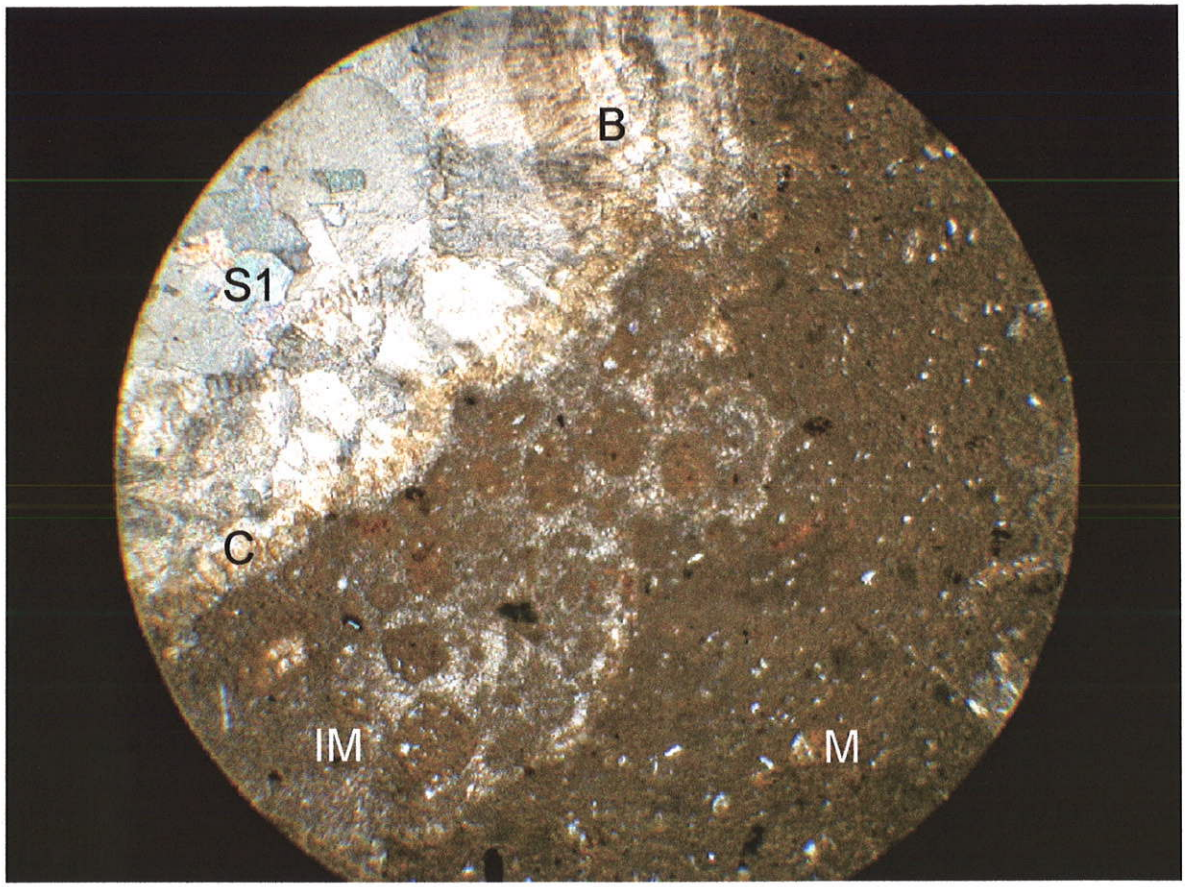

Figure 10. Diameter of view is 4.5mm. Paragenetic sequence of micrite (M), Intrapelmicrite (IM), yellow calcite (C), botryoids (B) and spar 1 (S1).

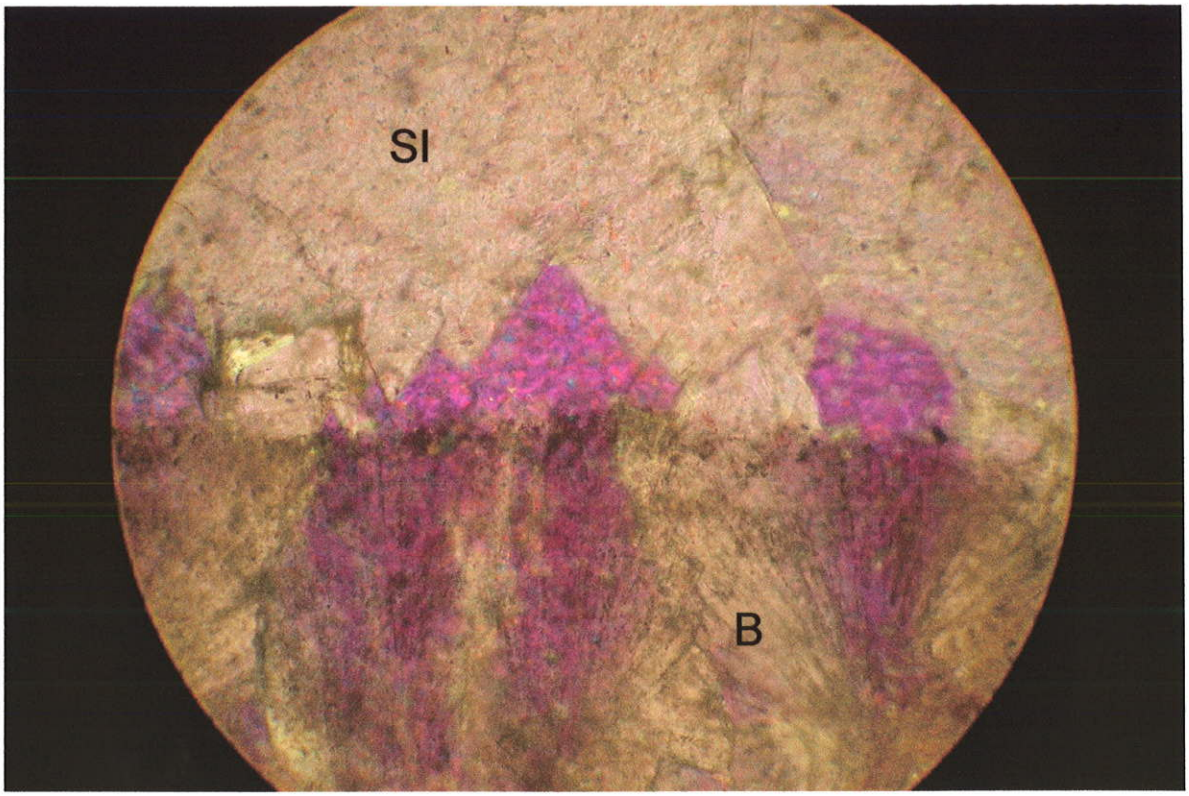

Figure 11. Botryoidal cement (B) showing optical continuity with spar 1 (S1) providing evidence for later sparitization. Diameter of view is 4.5mm. Photomirograph taken in cross polars with gypsum plate.

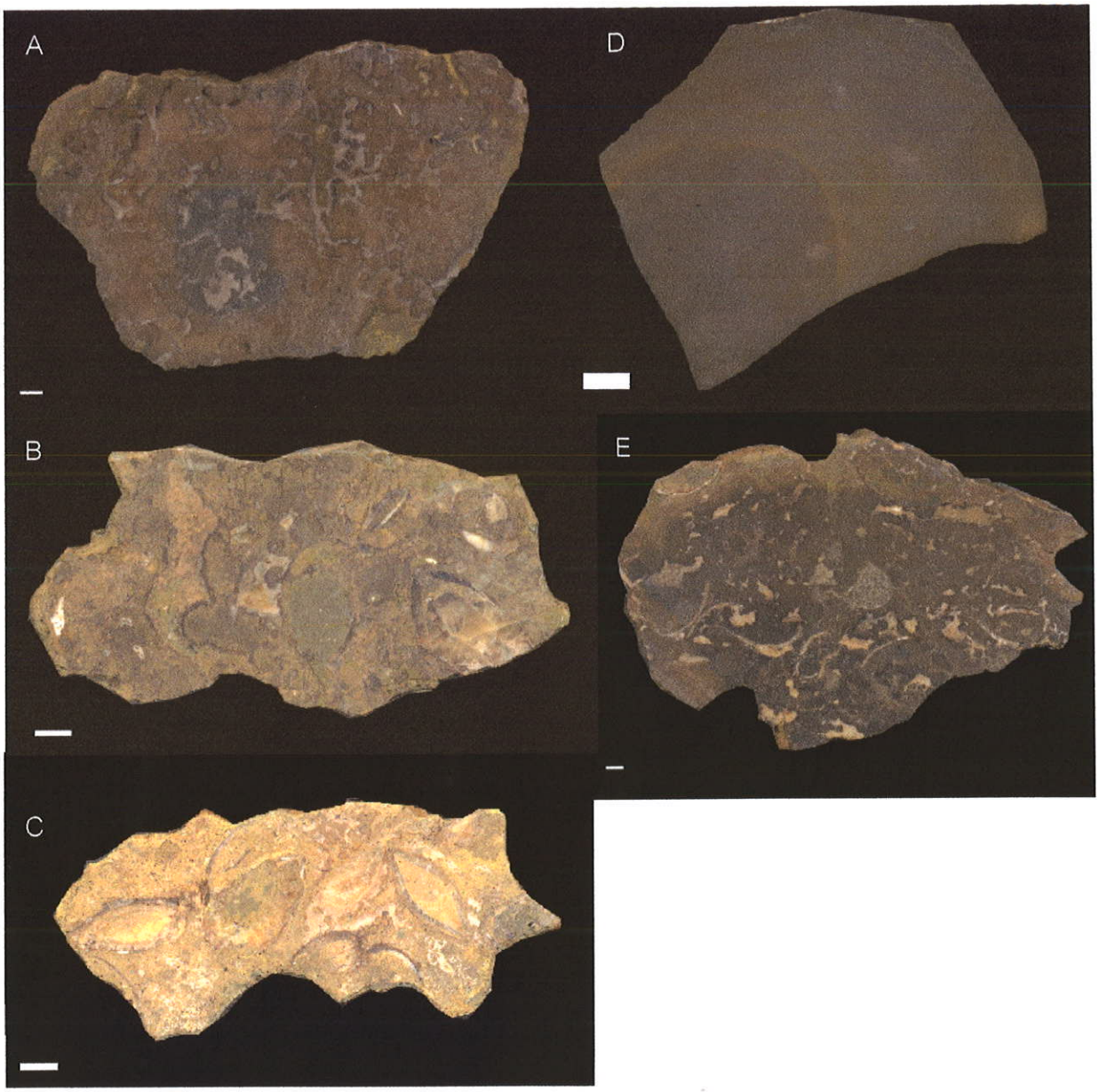

Fig. 12 Hand samples of each of the five lithofacies. Scale bars are 1 cm. (A) Lithofacies I. Abundant vugs with thick cement rinds, coarse calcite spar and few fossils. (B) Lithofacies II. Mostly articulated lucinids with some vugs. (C) Lithofacies III. Mostly abundant lucinid clams in micrite mud. (D) Lithofacies VI. Limestone concretions found generally in shale near carbonate shale interface. (E) Lithofacies V. Little to no fossil material with little to no early cement rinds around voids, interpreted as microbial activity.

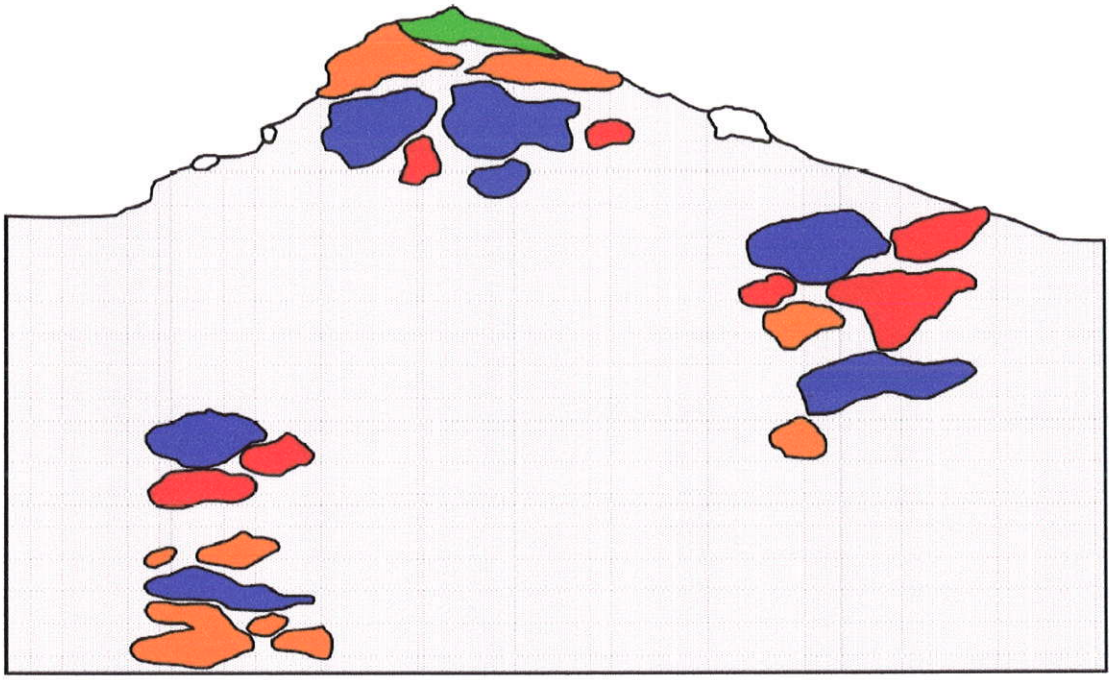

Figure 13. Lithofacies arrangement model. There is no clear pattern of butte development. The two carbonate clusters below the shale represent buttes at lower elevations. Lithofacies IV is not included as it was most often part of the shale shown here in white.

Facies I
Facies II
Facies III
Facies V

Table 1. Petrographic fabrics from each of the five lithofacies of the Tepee Buttes and their petrographic characteristics

Petrographic Fabric	Description	Crystal or Clast Size	Lithofacies occurrence	Cathodoluminescent character
Micrite	gray/brown, fine siliciclastic material 2%, sulfide material 5%	<0.4 mm	I,II,IV	Homogenous to mottled, dull dark orange
Pelmicrite	gray/brown, fine siliclastic material 5%, sulfides 1%, peloids	Peloids, 0.015-1mm	I, II, III	Homogeneous to mottled, dull dark orange
Intrapelmicrite	gray/brown, 1% fine siliciclastic material, 1% sulfides, peloids, intraclasts	Intraclasts, 0.1-3.25mm	I, II, III, V	Homogeneous, dull dark orange
Intrapelsparite	light gray, microspar, intraclasts, peloids, shell material	Spar, 0.15-1.5mm	I, II, III, V	Mottled, bright orange microspar
Yellow calcite cement	light to dark yellow, surrounds peloids, intraclasts and micrite, interlayered with the botryoidal cement	0.1-0.5mm	I, II, III, V	Homogeneous, dull orange to bright orange
Radial fibrous botryoidal cement	light gray to light tan, radiating out from yellow cement, rich bands of dark brown sulfide corrosion	0.3-1.25mm	I, II, III, V	Banding alternating bright orange to dark orange
Spar 1	Clear, blocky, pore filling, replacing earlier fabrics	0.25-1mm	I, II, III, V	Dark orange to nonluminescent
Late spar 2	Clear, blocky, occurring in fractures	0.3mm-1mm	I, II, III, V	Dark orange to nonluminescent

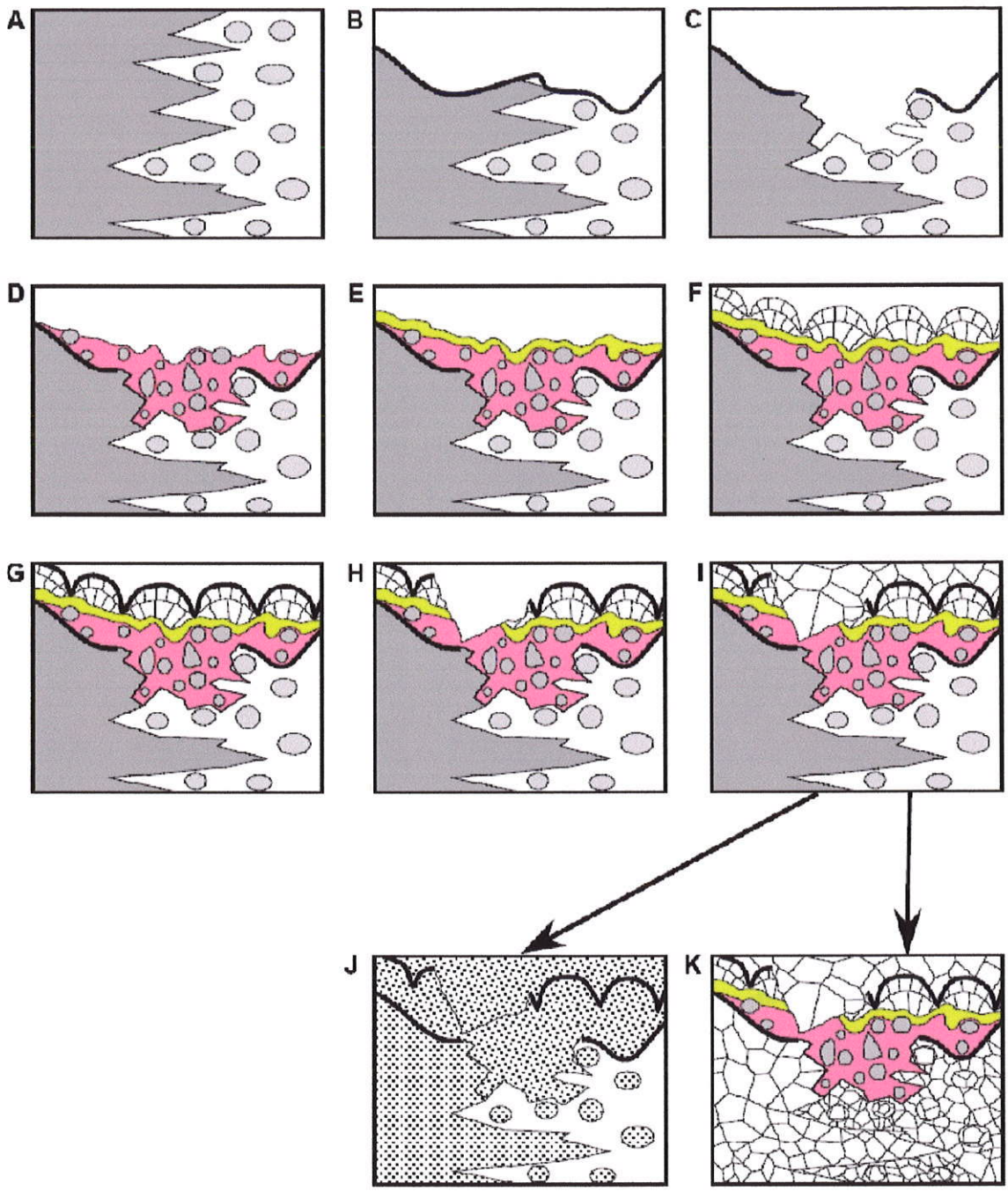

Fig. 14. Paragenetic and diagenetic sequence of formation and diagenesis in the Tepee Buttes Carbonates. (A) Formation of micrite and pelmicrite. (B) Corrosion of both fabrics. (C) Erosion into the corrosive event, micrite and pelmicrite. (D) Deposition and cementation of intrapeloidal fabrics (E) Yellow calcite cementation (F) Radial fibrous calcite cementation (G) Corrosion of radial fibrous calcite cement. (H) Erosion of the corrosive layer and the radial fibrous cements. (I) Spariatization of remaining void space. (J) Diagenetic micritization. (K) Diagenetic sparitization.

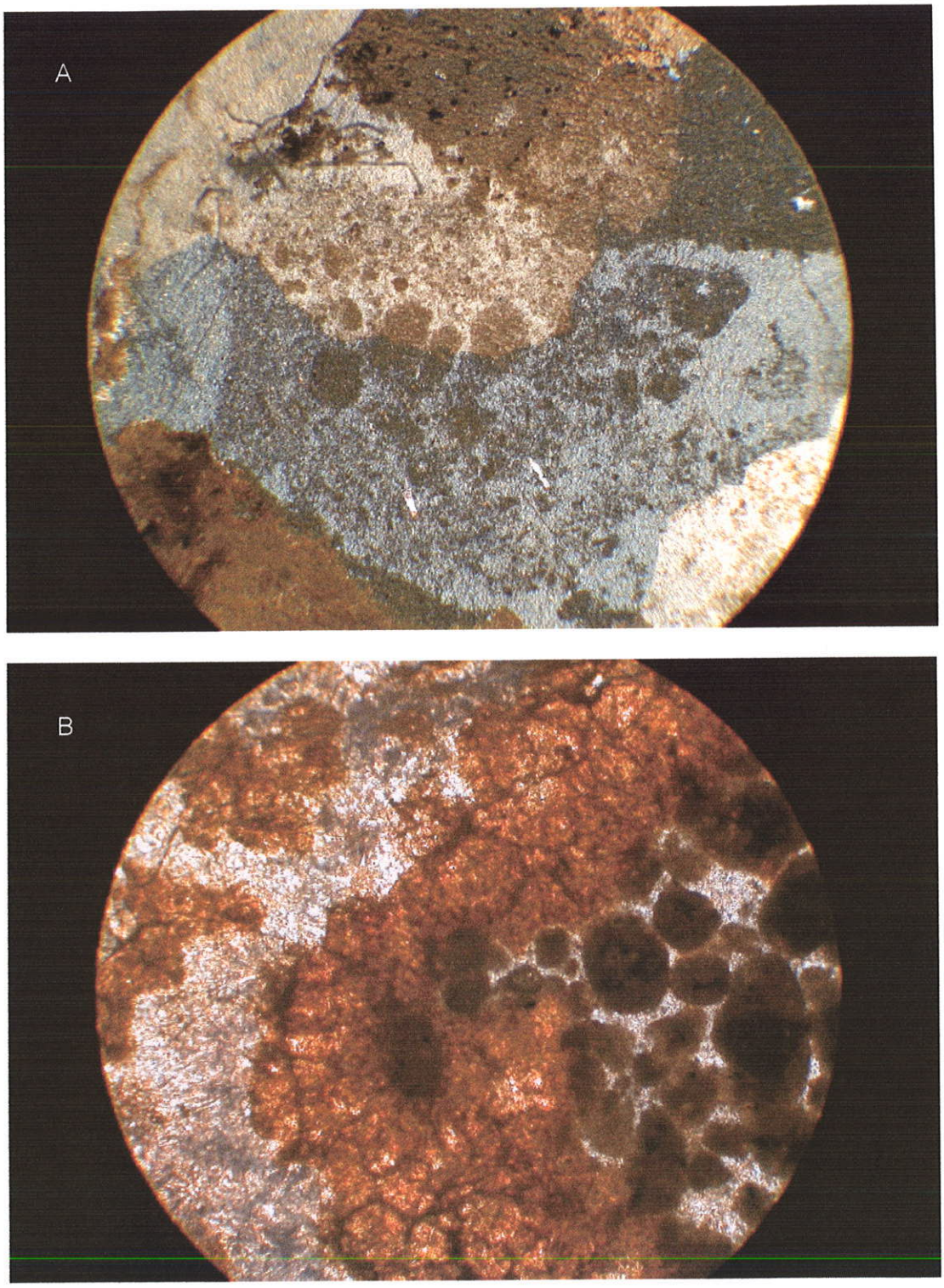

Fig.15. Photomicrogrpahs taken at 40X under cross polars. Scale is 4.5 cm across the view. A) Photomicrograph of diagenetic sparitization of the pelmicrite.
B) Photomicrograph of diagenetic micritization of the intrapelsparite, yellow calcite and the botryoids.